The Pennsylvania State University

The Graduate School

Department of Energy and Mineral Engineering

CHARACTERIZATION OF SURFACE FUNCTIONAL GROUPS ON CARBON MATERIALS WITH X-RAY ABSORPTION NEAR EDGE STRUCTURE (XANES) SPECTROSCOPY

A Thesis in

Energy and Mineral Engineering

by

Kyungsoo Kim

© 2010 Kyungsoo Kim

Submitted in Partial Fulfillment
of the Requirements
for the Degree of

Master of Science

December 2010

The thesis of Kyungsoo Kim was reviewed and approved* by the following:

Yongsheng Chen
Assistant Professor of Energy and Mineral Engineering
Thesis Advisor

R. Larry Grayson
Professor of Energy and Mineral Engineering

André L. Boehman
Professor of Fuel Science and Materials Science and Engineering

Caroline Burgess Clifford
Senior Research Associate, EMS Energy Institute

Yaw D. Yeboah
Professor of Energy and Mineral Engineering
Head of the Department of Energy and Mineral Engineering

*Signatures are on file in the Graduate School

ABSTRACT

Carbon materials have many applications due to their bulk or surface properties, and for the latter, surface functional groups play a decisive role. Many characterization techniques have been used to identify and quantify surface functional groups, but none is completely satisfactory so far especially when it comes to quantification. X-ray absorption near edge structure (XANES) spectroscopy has several advantages over the commonly used techniques, e.g., element specific, high sensitivity, characteristic spectra for different functional groups, and straightforward quantitative analysis. For oxygen functional groups on carbon materials, oxygen K-edge (543.1 eV) XANES is preferred over carbon K-edge (284.2 eV) since it minimizes the strong interference from the carbon substrate. Oxygen K-edge XANES was attempted over 13 years ago, but it was only partially successful with qualitative analysis due to spectrum distortion from charging effect because of poor sample conductivity. In this work, we collect oxygen K-edge spectra in both fluorescence yield (FY) and total electron yield (TEY) modes. Although relatively noisier, spectra collected in FY mode do not suffer from charging effect, which is very important for quantitative analysis by linear combination fitting. It is shown that an oxygen K-edge spectrum of oxygen containing functional group mainly consists of a pre-edge peak and a whiteline (the first intense post-edge peak). The XANES spectra are unique in the position and/or the intensity of the pre-edge peak and the whiteline. Thus, identification of different functional groups is possible by fingerprinting. By measuring known functional groups in reference compounds, it is determined that oxygen functional groups on carbon materials can be grouped into three categories. Each category consists

of a few functional groups, which have very similar XANES spectra, while significant difference exists between categories. Carboxyl-type groups include carboxyl, ester, and anhydride groups, and the features are a strong pre-edge peak at about 531 eV and a broad whiteline at 539 eV. Carbonyl-type groups include carbonyl and aldehyde groups, and the features are a strong pre-edge peak at below 530 eV and a broad whiteline at 539 eV. Hydroxyl-type groups include hydroxyl, phenol, and ether groups, and the features are no or very weak pre-edge peak at about 531 eV and a broad whiteline at 536-538 eV. Four activated carbons that underwent different treatments are analyzed by XANES. The relative total oxygen contents can be calculated from the edge step of their XANES spectra, and the identity and relative abundance of different functional groups are determined by fitting of a sample XANES spectrum to a linear combination of spectra of the reference compounds. It is concluded that oxygen K-edge XANES spectroscopy is a reliable characterization technique for the identification and quantification of surface functional groups on carbon materials.

TABLE OF CONTENTS

LIST OF FIGURES

LIST OF TABLES

ACKNOWLEDGEMENTS

I would like to express my gratitude to my advisor, Dr. Yongsheng Chen, who provided this great opportunity to work on the study. His valuable guidance, support, and encouragement ensured the completion of the work. His invaluable advice positively influenced not only my academic career, but also my life.

I would like to thank my committee members, Dr. R. Larry Grayson, Dr. André L. Boehman, and Dr. Caroline Burgess Clifford, for spending their valuable time editing and commenting on my thesis, which led to a higher quality of the final product.

There are people whom I should appreciate for their support. I am thankful to Dr. Xiaoliang Ma and Na Li for their help with preparing activated carbon samples, and TPD and DRIFTS analyses. I would also like to thank Dr. André L. Boehman for providing surface functional group reference compounds. My thanks also go to my friends in State College, who did not hesitate to provide precious advice. I would also like to thank all Energy and Mineral Engineering family for great support during my graduate school life.

I would like to express my special thanks to my family in South Korea. Without their love, endless support, and meaningful encouragement, this work could not be accomplished. Lastly, my beloved wife, Kalam Lee, who has been always on my side and supported me to finish this work, deserves my sincerest gratitude.

Chapter 1 Introduction

Carbon is a versatile material as it forms different structures and shows different properties. Some carbon materials are useful for their bulk properties. For example, diamond, the hardest naturally occurring material, is formed by sp^3-based carbon-carbon covalent bonds in a FCC structure in which the rigid carbon bonding network gives exceptionally hard characteristic. In contrast, graphite is a sp^2-based carbon material formed by parallel stacking of graphene sheets. Since the sheets are connected by relatively weak van der Waals forces, graphite shows soft characteristic and is used as a solid lubricant [1,2]. Graphite is also used as an electrode material due to its electrical conductivity. The delocalized valence electrons on a graphene layer can move freely within the layer, and these valence electrons conduct electricity. Carbon nanotubes can be used for field electron emission, energy storage, and atomic force microscopy due to their cylindrical conformation, exceptional mechanical strength, and thermal and electrical conductivity [3,4]. Carbon nanofibers can be used for material reinforcement and hydrogen storage for their strong individual structure and availability to produce various conformations [5,6]. While carbon nanotubes show ballistic electron transport [7,8], carbon nanofibers conduct electron along their sidewalls [9-12]. Having unique graphitic multi-layer with hollow center morphology, carbon nano-onions are good solid lubricant and possible protector for air sensitive materials [13].

Some carbon materials are used for their surface properties. For example, activated carbon can be used as absorbent and catalyst support. Surface functional groups

play a very important role in shaping the surface properties of the carbon materials. Extensive efforts have been devoted to controlling the surface functional groups in order to prepare the materials for certain applications. On one hand, physical and chemical methods are developed to create and modify the surface functional groups. For instance, the inert and hydrophobic surface nature of carbon nanotubes is a major obstacle to their various applications, and attachment of oxygen functional groups to the surface can solve the problem as it enhances the wettability of the carbon nanotube to polar solvents; this produces more reactive surfaces [14-17]. In addition, the surface area and pore volume of carbon nanofibers can be increased by oxidation with strong oxidizing agents. This improves the use of carbon nanofibers as catalyst support [18]. The weak interfacial interactions between carbon nanofibers and polymers when producing reinforced materials can also be solved by forming oxygen-containing compounds on the surface [19,20]. Moreover, many different oxidizing methods for activated carbons have been developed to improve the adsorptive behavior of activated carbon toward specific pollutants such as cadmium and copper [21-23]. The surface functional groups which may exist on carbon materials include carboxylic acid/anhydride, carbonyl, ether, ester, aldehyde, pyrone, and hydroxyl groups. The structures of these functional groups are presented in Figure 1.1 [24]. By using different oxidizing agents, different types of surface functional groups may be created on carbon materials. Figures 1.2 and 1.3 show the results of carbon nanofiber surface modification by nitric acid and maleic anhydride respectively [19,20]. In both cases, the formation of different oxygen-containing compounds is observed. Carbon nanofiber modified by nitric acid forms ester, anhydride, quinoid and phenolic hydroxyl and the modified carbon nanofibers show improved

wettability to water. Surface modification by maleic anhydride forms anhydrides on the surface and the formed anhydrides build bridged structure with hydroxyl groups. When this modified carbon fiber is further reacted with nitric acid, more bridged structure is formed and this improves the interaction between carbon nanofiber and imide structure, which is helpful for producing a reinforced polyimide matrix composite. On the other hand, many characterization methods have been used to identify and quantify the surface functional groups in order to establish the relationship of the surface properties and functional group(s), to understand the working mechanism of carbon materials, and to develop better carbon materials for various applications. However, proper characterization of the surface functional groups still remains a challenging problem due to their nature (low overall content coupled with the presence of multiple species).

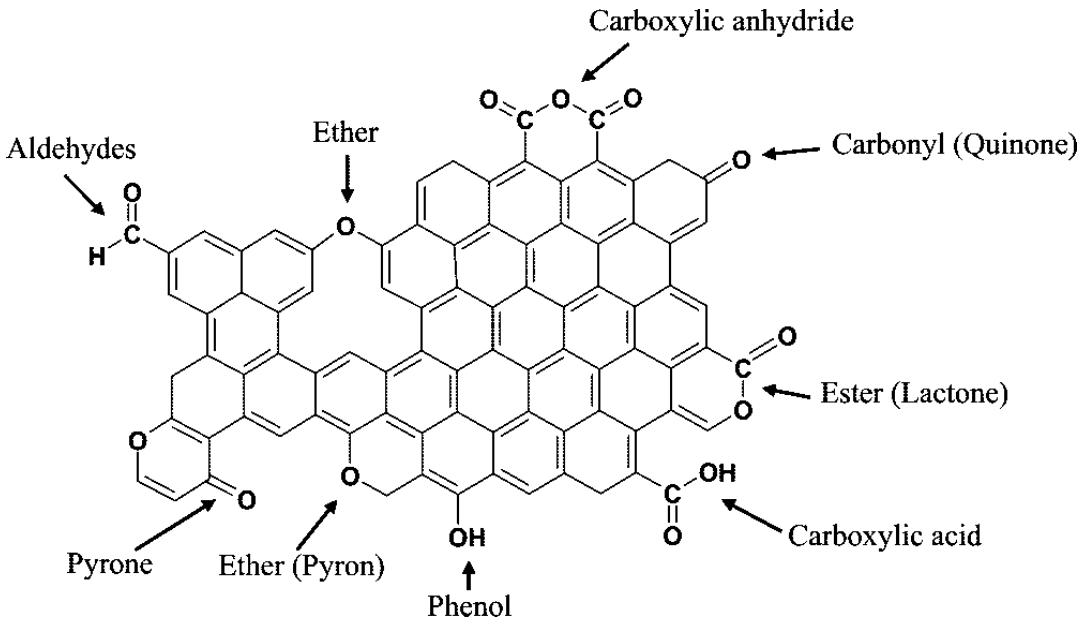

Figure 1.1. Oxygen functional groups on the surface of carbon materials (figure taken from Kundu et al. [24]).

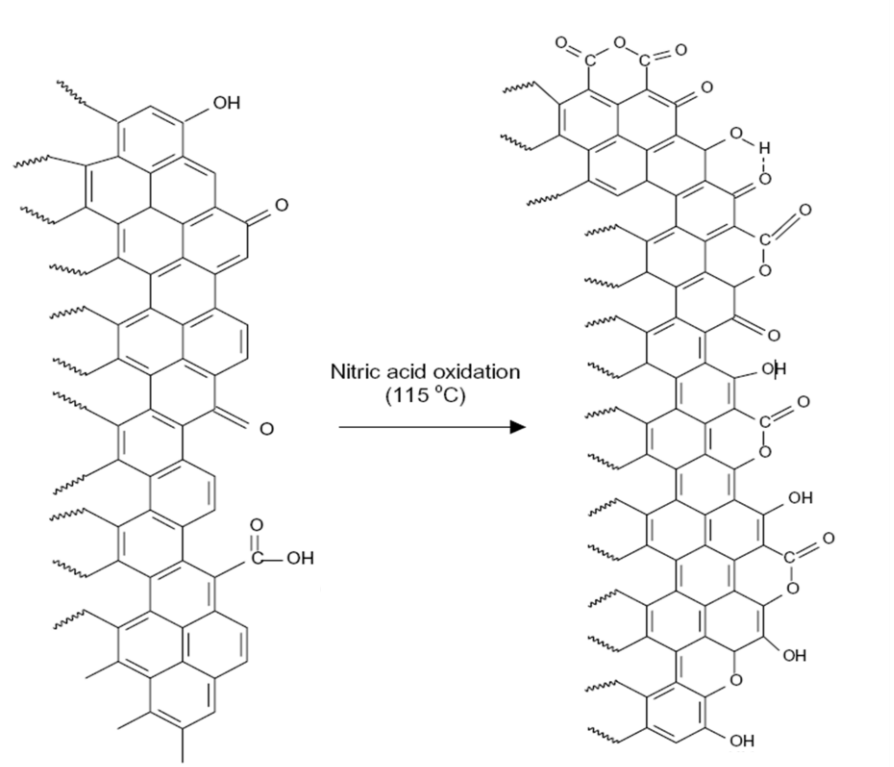

Figure 1.2. Schematic of the formation of new surface functional groups on carbon nanofiber by nitric acid oxidation (figure taken from Lakshminarayanan et al. [19]).

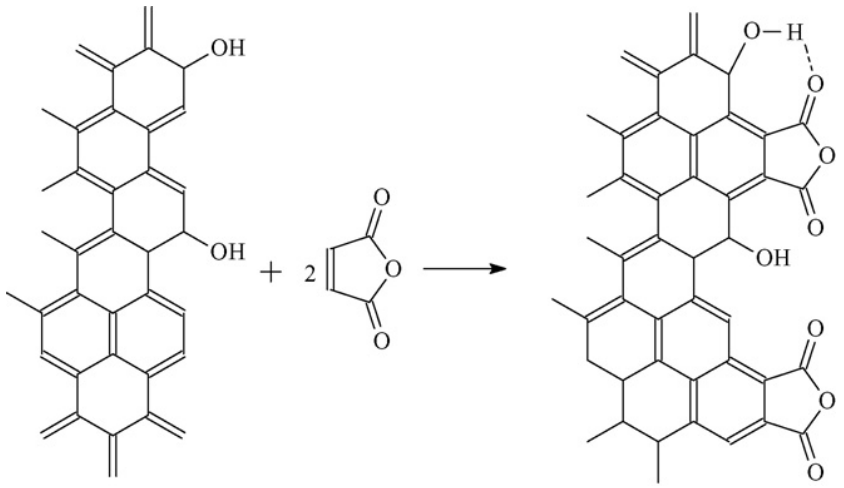

Figure 1.3. Schematic of the formation of new surface functional groups on carbon nanofiber by maleic anhydride (figure taken from Lu et al. [20]).

Among the various techniques that have been used for the characterization of surface functional groups, x-ray photoelectron spectroscopy (XPS), infrared spectroscopy (IR), temperature-programmed desorption (TPD), and titration are the most common techniques. Boehm compared these techniques in great details in a review paper [25]. Although all these techniques give useful information about carbon materials and their surface functional groups, each technique has its own limitations, and proper identification and reliable quantification of surface functional groups are still not completely satisfactory. In XPS, quantification usually involves deconvolution of overlapping peaks, which is somewhat arbitrary as peak position, peak shape, and peak width are assumed for different species and the assumptions are difficult to verify [25]. If the analysis is performed based on C 1s spectra, a strong interference from the carbon substrate is expected since C-C species are dominant. Moreover, charging of carbon materials, which is not uncommon, may cause peak distortion and add more uncertainties in the analysis. In IR, each peak contains multiple contributions from different chemical bonds, which significantly hinders proper peak assignment. The low concentration of surface functional groups on carbon materials causes the carbon substrate to dominate IR spectrum, which makes both qualitative and quantitative analyses of surface functional groups difficult [24,26]. TPD depends on evolved gases such as CO and CO_2 from surface functional groups for identification and quantification purposes, however, a single functional group may result in multiple gases and there is possibility of secondary reactions, which bring uncertainties to the TPD analysis [25]. In addition, TPD analysis also involves deconvolution of overlapping peaks, which has the same problem faced by

XPS. Titration is based on the acidic and basic properties of surface functional groups. However, titration can only detect surface functional groups in a certain p*K*a range, offering limited information about surface functional groups [25,27]. Due to the low sensitivity, titration method requires a large amount of sample, which limits the use of titration for the study of surface functional groups [28].

X-ray absorption near edge structure (XANES) spectroscopy is a technique that can potentially overcome the limitations faced by the commonly used techniques. XANES is an element specific technique that probes local electronic structure around a specific element of interest. By performing oxygen K-edge XANES, the interference from carbon in the substrate can be avoided [29]. In addition, intense synchrotron x-ray radiation provides high intensity which allows the detection of very low level of surface functional groups [30]. Moreover, surface functional groups may have unique XANES spectra, by which qualitative analysis is possible by fingerprinting [31]. Both carbon and oxygen K-edge XANES works have been reported in the literature for characterization of surface functional groups [31-35]. Carbon K-edge XANES spectroscopy has been used to characterize chemical structure of carbon, and often as a minor component of the material, surface functional groups are identified as well. Methods have been developed to quantify different carbon species including deconvolution of overlapping peaks. Uncertainties may result from the fact that the surface functional groups in most cases are minor components compared to the dominant contribution from other species in the substrate that do not contain oxygen such as C-C and C-H bonds. To overcome these problems, it seems that oxygen K-edge XANES spectroscopy is a convenient choice since only oxygen containing surface functional groups will be detected and no

interference from other species in the substrate is expected. In addition, reference compounds with only one type of functional groups are widely available, thus obtaining reference spectra of different functional groups would not be an issue. Surprisingly, there are only few reports in the literature on oxygen K-edge XANES works, and they are limited to qualitative analysis [31,36]. The main reason is believed to be charging effect that distorts the XANES spectra of poorly conducting carbon materials when the spectra are collected in total electron yield mode. In the present work, fluorescence yield mode is used to collect oxygen K-edge XANES spectra, which effectively overcomes the charging effect. We obtain XANES spectra of reference compounds for individual functional groups and use linear combination fitting method to identify and quantify the functional groups present in four activated carbon samples. Relative total oxygen contents in the activated carbon samples are calculated from the difference in absorption before and after the edge (or edge step). TPD and DRIFTS analyses are also performed to show the limitations that these techniques face when used for the characterization of surface functional groups. It is shown that oxygen K-edge XANES spectroscopy is a reliable tool for identifying and quantifying different surface functional groups on carbon materials.

Chapter 2 Literature Review

2.1 Characterization Methods for Surface Functional Groups

Among a variety of analytical techniques, X-ray photoelectron spectroscopy (XPS), infrared spectroscopy (IR), temperature-programmed desorption (TPD), and titration are the most commonly used techniques to characterize the surface chemistry of carbon materials. All these techniques give useful information about carbon materials and their surface functionality.

2.1.1 X-ray Photoelectron Spectroscopy (XPS)

X-ray photoelectron spectroscopy (XPS) is a technique which measures electron binding energies of an atom. In XPS, an electron is excited to the vacuum energy level and becomes a free electron by absorbing X-ray energy higher than its binding energy [37]. This phenomenon is called the photoelectric effect, and the free electrons are referred to as photoelectrons. The binding energy of the original electron, which is characteristic of the atom and the electron shell where the electron was ejected, is determined by subtracting the kinetic energy of the photoelectron and work function of the spectrometer (work function is the minimum energy needed to remove an electron from a solid to a point immediately outside the solid surface) from the energy of the X-ray beam,. The electronegativities of neighboring atoms also affect the binding energy to some degree. As a result, XPS detects the elements in a sample, and also contains information about their chemical environments. In some cases, the difference in binding

energy is small corresponding to the bonding situations. Therefore, deconvolution of peaks is required in order to retrieve the chemical information [25].

Common X-ray energies used in XPS are 1253.6 eV (Mg Kα) and 1486.6 eV (Al Kα). The photoelectrons have energies less than the source, and at these energies the photoelectron can travel only a few nanometers before losing their identities and contributing to the background [37]. Consequently, XPS measures elements from the surface (about 5-15 nm), which makes it useful for the identification of surface functional groups and their relative concentrations [27]. However, there are disadvantages when XPS is used for the analysis of surface functional groups on porous carbon materials. For example, in most mesoporous carbon materials, a large fraction of surface area is in pores, so not all surface functional groups are accessible by XPS and additional characterization methods such as TPD and titration are needed to observe the functional groups inside the pores [38]. More importantly, deconvolution of overlapped peaks is hindered significantly by the close proximity of binding energies, which makes accurate qualitative and quantitative analysis difficult [25,39]. Figure 2.1 shows C1s XPS spectrum of some oxidized carbon fiber. Deconvolution of the original spectrum was performed to identify and quantify different functional groups [5]. For deconvolution of overlapping peaks, different peak shapes are assumed for different carbon structures. For instance, for graphite-like structure, asymmetric peak is required, and for aliphatic structure, Gaussian peak is needed [40]. Peak position and peak width are also assumed, making spectral analysis somewhat arbitrary. Similar binding energies of different carbon surface functional groups make peak deconvolution more difficult [41]. In Figure 2.1, the dominant peak at 284.5 eV is attributed to the carbon substrate (graphitic carbon). The

peaks corresponding to surface functional groups are small shoulder and tail superimposed on the major peak, which visually manifests the difficulties in peak deconvolution. To ease this problem to some extent, chemical tagging of surface functional groups by selective reaction with specific compounds has been used to achieve more reliable peak deconvolution. For example, hydrogen atom in hydroxyl groups can be replaced with a fluorine compound through a reaction with trifluoroacetic anhydride (TFAA). Since fluorine has a high sensitivity for XPS analysis, detection of hydroxyl group can be achieved more easily [26,42].

In XPS, a calibration process is required since charging of materials can affect the kinetic energies of photoelectrons [25]. Charging effect is caused by surface charging-up of a material with poor conductivity. This charging of samples may cause peak distortion, making both qualitative and quantitative data analyses difficult [43]. In addition, XPS is performed in high-vacuum condition, which differs from the real condition where carbon materials are usually used. Therefore, in reality, surface rearrangement of carbon materials can occur especially when the porous surface structure is easily oxidized by aging. This hinders understanding the role of surface functional groups on the properties of carbon materials [27].

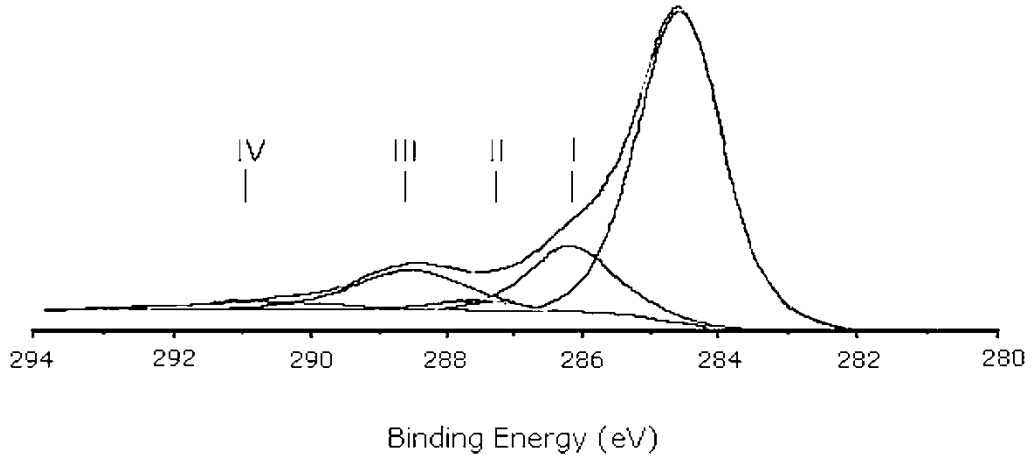

Figure 2.1. Deconvolution of XPS spectrum of oxidized carbon fiber: (I) phenols, (II) carbonyls, (III) carboxyls, (IV) carbonate (figure taken from Yue et al. [5]).

2.1.2 Infrared Spectroscopy (IR)

Infrared spectroscopy (IR) is a technique that measures the vibrations of a molecule or functional group. In IR spectroscopy, a molecule absorbs light that induces vibrational excitation of covalent bonds of the molecule [37]. A molecule can have various vibrational modes which are characteristic of its components. Since the energy of the absorbed light corresponds to these vibrational modes, it is possible to determine the structure of a compound with IR. For example, IR can identify carboxylic groups in a compound by C=O stretch and O-H stretch bands at ~1730 cm^{-1} and 3234 cm^{-1} respectively. Therefore, the unique IR spectrum of a compound (unique peak position, intensity, and shape) due to unique configuration of covalent bonds existing in the compound allows qualitative analysis of unknown materials by fingerprinting.

However, there are some disadvantages of IR when applied to surface functional group analysis. Firstly, the accurate assignment of absorption bands is hard to achieve

because IR measures the absorption by different molecules simultaneously. As a result, an absorption band may contain contributions from not only surface functional groups, but also carbon substrate, which allows only limited qualitative and quantitative analyses [26]. For example, peaks at 900-1300 cm^{-1} with a maximum peak at 1116-1143 cm^{-1} is usually found in both oxidized carbons and phosphoric acid activated carbon. The diversity of oxygen and phosphorous compounds in this area makes the clear distinction of the peaks difficult [44]. Figure 2.2 shows FTIR spectra of carbon nanotubes that were processed by different oxidizers and under different conditions. Both samples (a) and (b) were oxidized by dry air first and treated with HCl and HNO_3, respectively. Sample (c) was oxidized by H_2O_2 and treated with HCl.[45]. The band at ~1100 cm^{-1} in (c) is assigned to C-O stretching. The broad bands at 3234 cm^{-1} and 3412 cm^{-1} in (b) are assigned to O-H stretching in carboxylic acid group and hydroxyl group, respectively. The ~1730 cm^{-1} band comes from C=O stretching in carboxylic acid group. However, the author suggests that the band at 1230 cm^{-1} in (b) may come from O-H bending mode or C-O stretching mode, and the bands near 1400 cm^{-1} are unknown. This shows difficulties in peak assignment. Secondly, due to the low concentration of surface functional groups on carbon materials, the peaks from substrate and other molecules can dominate the IR spectrum. Therefore, detection sensitivity can be an issue for IR in terms of total oxygen content, and quantitative analysis of IR data is essentially not possible [24,26].

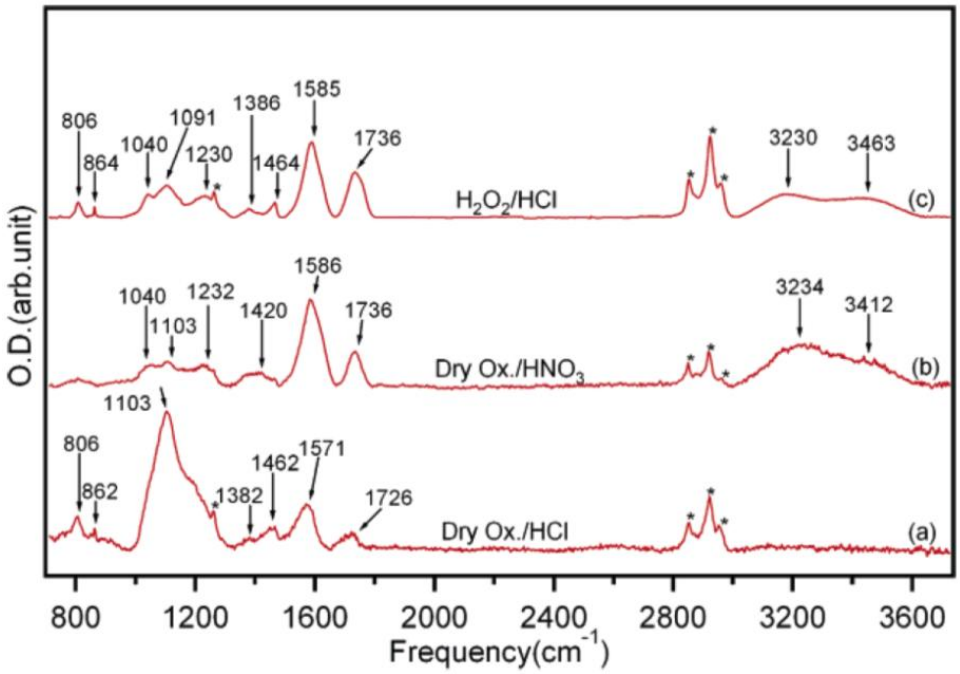

Figure 2.2. FTIR spectra of differently processed carbon nanotubes (figure taken from Kim et al. [45]).

2.1.3 Temperature Programmed Desorption (TPD)

Temperature programmed desorption (TPD), also known as thermal desorption spectroscopy, allows the observation of evolved gases from a material. When carbon materials are heated with a constant heating rate in a vacuum or in a flowing helium environment, surface functional groups decompose to give CO, CO_2, H_2, or, H_2O at different temperatures depending on their thermal stability. For example, CO_2 is evolved from carboxylic groups at low temperatures while other functional groups still remain stable. A mass spectrometer, such as a quadrupole mass spectrometer, is needed to analyze the evolved gases. TPD provides quantification and thermal stability investigation of surface oxygen functional groups [46].

However, there are some drawbacks in TPD analysis. Firstly, close decomposition temperatures of different functional groups cause peak overlapping, making peak assignment difficult [26]. Figure 2.3 shows TPD spectrum of oxidized carbon nanofiber [47]. Although the spectrum shows the presence of different surface functional groups (carboxyl, anhydride, peroxide, and lactone), deconvolution of overlapping peaks is somewhat arbitrary as in XPS. Secondly, some functional groups can produce multiple evolved gases, which hinders proper qualitative and quantitative analyses. For example, a cyclic lactone can produce either two molecules of CO or one molecule of CO_2, and these reactions can take place simultaneously [25]. Thirdly, there are also possibilities for secondary reactions. For instance, collision of CO with oxygen on the surface of a material can form CO_2, and CO_2 may also be generated from two CO molecules by hitting the pore walls of a sample due to the slow diffusion of the evolved gases in narrow pores [25]. Lastly, TPD peak assignments in the literature sometimes differ from different research groups. This is partly because TPD results can be influenced by the pore structure of the materials, the experimental set-up, and the experiment conditions such as heating rate, sample mass, and gas flow rate [24,40]. New deconvolution methods with a multiple Gaussian function have been developed to achieve more reliable peak deconvolution [27,47].

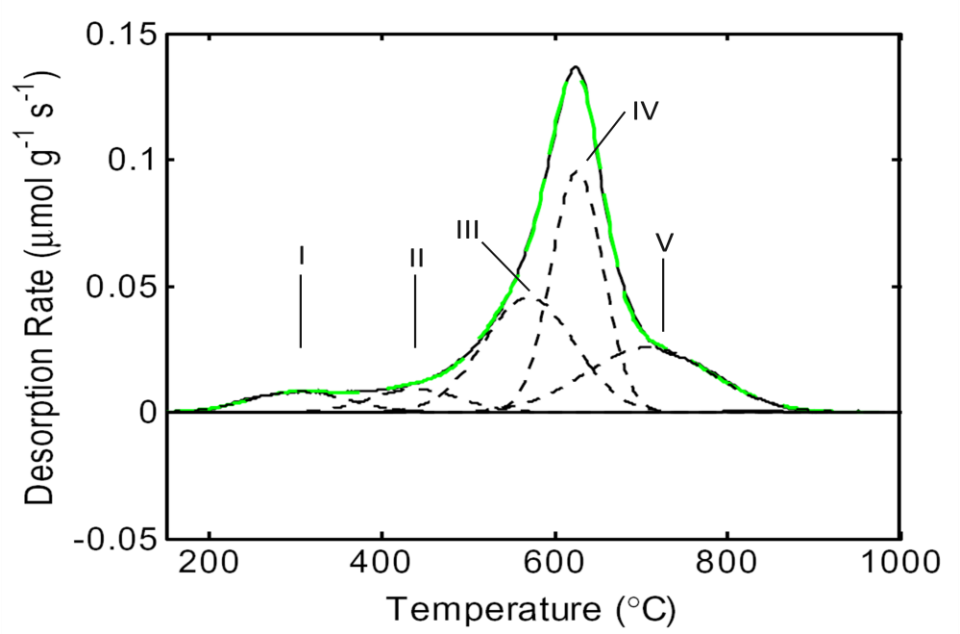

Figure 2.3. TPD spectrum of oxidized carbon nanofiber: (I) carboxyls, (II) carboxylic anhydrides, (III) peroxides, (IV) and (V) lactones at different sites (figure taken from Zhou et al. [47]).

2.1.4 Titration

Titration provides information about the concentrations of certain functional groups in a sample. In this method, a reagent with a known concentration and volume reacts with a solution of the analyte with unknown concentration until the reaction reaches an endpoint. At the endpoint, the reaction reaches equilibrium, and the concentration of the analyte can be calculated from the volume of consumed reagent [25]. There are different methods to measure the endpoint of a reaction. For example, phenolphthalein is used in acid-base titrations as it changes its color from colorless to pink at certain pH (8.2 or higher). In some redox titrations, there is no need of indicator since the color of the solution changes as the oxidation states of the reactant changes.

Titration can be applied for the study of carbon surface functional groups by analyzing their acidic and basic properties. For example, carbonyl groups, lactones, and lactols are the main causes of the acidic properties of carbon surface. Since each group has different acidities, they can be distinguished from each other by neutralizing them with different basic compounds such as NaOH, Na_2CO_3, and $NaHCO_3$. Although the acidic property of a functional group is influenced by its chemical environment, the charge of dissociated compounds around it, and the position of other functional groups, the differences in acidity among surface functional groups are large enough to distinguish them by titration method [25]. A titration result of HNO_3 activated carbon is presented in Figure 2.4 [48]. Four peaks with maxima at 4.1, 5.3, 7.6, and 9.9 are identified from the analysis. First three peaks are ascribed to carboxyl acids and the last peak is assigned to phenolic groups. The small shoulder at 8.9 is also observed, but not identified.

Although titration allows qualitative and quantitative analyses of carbon surface functional groups, it has several drawbacks. Firstly, it is time-consuming to reach equilibrium during the analysis especially in microporous materials. This is due to slow diffusion caused by narrow pores [27]. Secondly, titration is available only for the functional groups in a certain p*K*a range because outside the range water behaves as a buffer solution which reduces pH change of the solution when strong acid or is base added [25,27]. Thirdly, due to low sensitivity of titration method, it requires a large amount of sample [28].

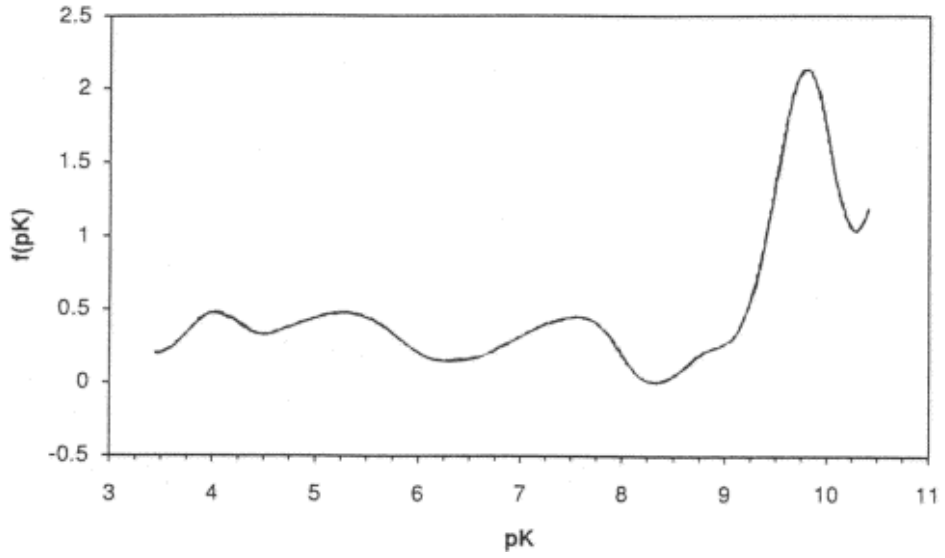

Figure 2.4. Acid constant distribution of an oxidized activated carbon (figure taken from Bandosz et al. [48]).

In summary, many techniques have been used for characterization of surface functional groups on carbon materials. However, each technique has its limitation, and proper identification and reliable quantification of surface functional groups are still not completely satisfactory. As a result, modifying surface properties by controlling surface functional groups becomes inefficient due to lack of means to monitor the changes. For example, the measurement of the adsorption performance of activated carbons is based on trial and error because it is difficult to identify and quantify the changes in surface functional groups caused by oxidation, which significantly hinders development of efficient adsorption methods [26]. Therefore, it is of most importance to understand the relationship between the surface chemistry and the behavior of carbon materials in many important processes, which allows the determination of the types and concentrations of oxygen functional groups for specific applications. Complete identification and

quantification of the surface oxides with proper characterization methods play a significant role in achieving this goal.

2.2 X-ray Absorption Near Edge Structure (XANES) Spectroscopy

2.2.1 Basic Concept

X-ray absorption fine structure (XAFS) spectroscopy measures the X-ray absorption of a material as a function of energy. When the X-ray energy is just enough to free electrons from a certain element in the material, a sudden increase in the absorption is observed, which is referred to as an absorption edge in XAFS. Absorption edge is labeled based on the electron shell in which electrons that absorb X-rays are located [49]. For instance, when an absorption edge stems from X-ray absorption by K-shell electrons in oxygen atoms in a material, the absorption edge is called oxygen K-edge. After absorption edge, absorption usually decreases with increasing energy. Fine structure in absorption exists near absorption edge. XAFS spectrum can be roughly divided into two different regions: XANES (X-ray absorption near edge structure) and EXAFS (extended X-ray absorption fine structure). XANES refers to the region ± 50 eV from the absorption edge. XANES region consists of the absorption by bound-state electron transition from core level to unoccupied valence orbital (pre-edge peak), and the absorption by electron transition above the Fermi level (whiteline) [49]. In XANES, because the ejected photoelectron has low kinetic energy, it experiences multiple scattering by neighboring atoms. This causes intense X-ray absorption XANES. XANES is dependent on the

electronic structure around an atom which is directly related to bond types and bonding situation with neighboring atoms. XANES gives information about oxidation state and coordination environment of an atom [29,51]. The sensitivity of XANES to oxidation state and coordination environment of an atom results in unique XANES spectrum, which makes qualitative analysis possible by fingerprinting. EXAFS is the region after XANES and it extends far beyond the XANES region (40 to 1500 eV). In EXAFS, only a small fraction of the ejected photoelectron is back scattered due to high kinetic energy, and this causes fine structure in EXAFS region. EXAFS provides information about bond distance to neighboring atoms, coordination number, and chemical identity of neighboring atoms [52,53].

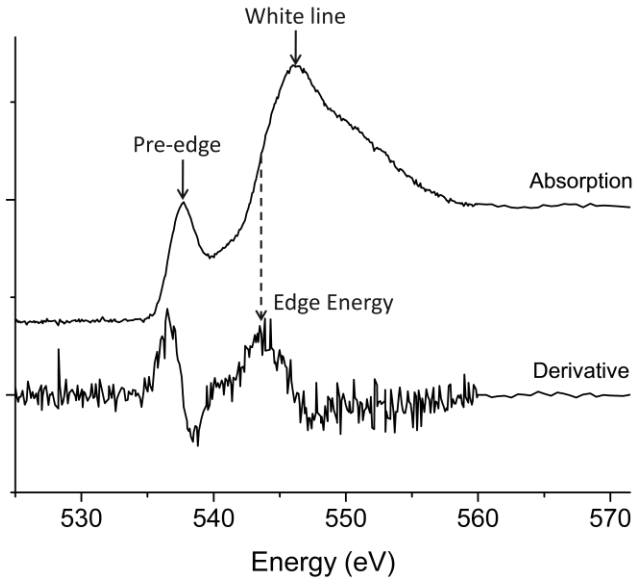

Figure 2.5. Oxygen K-edge XANES spectrum of an activated carbon and its first derivative

Figure 2.5 shows oxygen K-edge XANES spectrum of an activated carbon and its first derivative. The first inflection point of the main peak (544 eV) is the K-edge position

(absorption edge energy) where transition of the 1s electron to the first empty level above the Fermi level occurs. The peak before the absorption edge is pre-edge peak. The regions before pre-edge peak and after main peak are called pre-edge and post-edge respectively.

2.2.2 Collection Methods

2.2.2.1 Transmission

There are three collection methods for XANES spectroscopy: transmission, fluorescence yield, and total electron yield modes. In transmission mode, absorption is measured by ln (I_0/I), where I_0 is the intensity of incident X-ray and I is the intensity of X-ray coming out of the sample [49]. To obtain good results from transmission, samples have to be thin enough to allow X-ray to transmit. The optimal sample thickness is a function of sample composition and X-ray energy. For example, at the oxygen K-edge, the thickness of the carbon sample has to be less than one micron. Thus, it would be very difficult to measure oxygen XANES in transmission mode.

2.2.2.2 Fluorescence Yield

When an electron gets excited by an X-ray beam, the excited electron moves up to an unoccupied higher energy level, or goes out of the atom. In both cases, a hole is created. The created hole is then filled by electron in higher energy state. In the process, the energy difference between the two energy states is released either radiatively (by

emitting fluorescence) or non-radiatively (by emitting Auger electrons) [37]. Fluorescence yield counts the emitted fluorescence photons from a sample as a function of X-ray beam energy. By dividing fluorescence yield data by incident X-ray intensity (I_0), X-ray absorption is calculated [49]. Fluorescence is useful especially for the bulk analysis of a sample because the penetration depth of incident X-ray is relatively deeper. However, fluorescence yield signal may be reduced when observing a highly concentrated sample because the incident X-ray and fluorescence radiation can be absorbed by the sample. This phenomenon is called self absorption [54]. On the other hand, dilute samples have less number of elements causing a self absorption problem, and therefore there is less chance of signal reduction. Since the concentration of surface functional groups is very low, there is no significant self absorption problem in the data collected in this work. In addition, when observing lighter elements such as carbon and oxygen, data from fluorescence yield have low signal to noise ratios since non-radiative relaxation (Auger process) is dominant in lighter elements. Therefore, more scans and more time are needed to obtain good quality data.

2.2.2.3 Total Electron Yield

Total electron yield collects secondary electrons, and the signal is dominated by Auger electron due to its higher kinetic energy [49]. By dividing total electron yield data by incident X-ray intensity (I_0), X-ray absorption is calculated. The spectra from this method carry information about the surface of a sample because many secondary electrons from deeper energy levels lose their energy through collision with other

electrons while escaping from the sample. Therefore, the secondary electrons from only a certain depths can reach the detector. The advantage of the method is that it does not experience the signal reduction as fluorescence yield. Since the penetration depth of total electron yield is much lower, there is less chance that the attenuation of incident X-ray occurs. However, charging of samples sometimes distorts the spectra especially when dealing with less conductive samples, which florescence yield does not suffer from [43].

2.2.3 XANES for Characterization of Surface Functional Groups

While almost all the characterization techniques have limitations on the investigation into carbon surface functional groups, XANES spectroscopy has significant advantages over other techniques. For instance, XANES is an element specific technique that probes local electronic structure around a specific element of interest, which prevents interferences from other elements that sometimes can be dominant in the sample [49]. XANES spectra of different functional groups are unique, which makes qualitative analysis possible by fingerprinting. Information about relative abundance of surface functional groups within a sample can be obtained by performing linear combination fitting of sample spectra with spectra of standard materials. In addition, intense synchrotron X-ray radiation provides high intensity which allows the detection of very low level of surface functional groups [49].

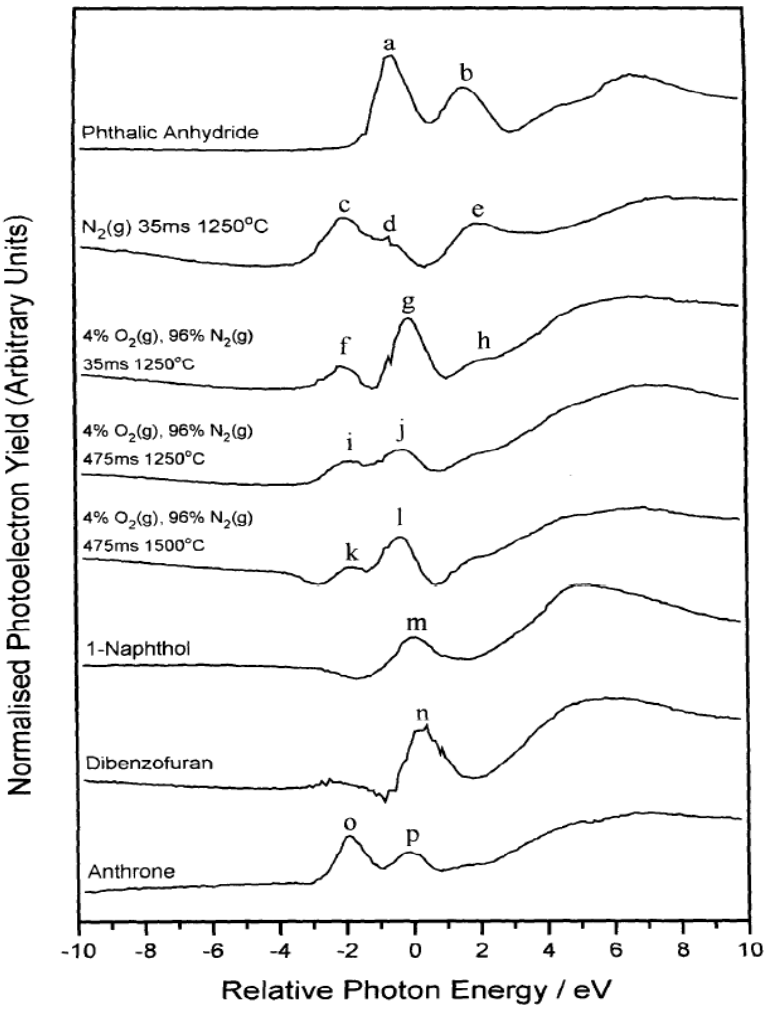

Figure 2.6. Oxygen K-edge XANES spectra of char samples combusted at different conditions. Surface functionality reference compounds are included for comparison (figure taken from Turner et al. [31]).

Figure 2.6 shows oxygen K-edge spectra of char samples combusted at different conditions [31]. The work was done by a group of researchers about 13 years ago. The spectra were obtained in total electron yield mode. The samples other than char samples are oxygen functional group reference compounds which were used for qualitative analysis. The spectra of the standards are different, thus, it is possible to identify different functional groups in the samples. However, the spectra are distorted by charging effect of

carbon substrate, and quantification of different surface functional groups is not possible. When oxygen K-edge XANES is measured on oxidized carbon materials, an X-ray beam excites a small fraction of electrons in carbon substrate as well as surface functional groups, producing secondary electrons. If the carbon substrate has low electrical conductivity, the holes in the carbon substrate produced by ejecting secondary electrons cannot be filled, causing the carbon substrate to be positively charged. As a result, the positively charged carbon substrate attracts the secondary electrons coming out of the oxygen atoms in the surface functional groups, and therefore, spectra measured in total electron yield mode get distorted [55]. In contrast, fluorescence yield mode, does not suffer from charging effect since it measures X-ray radiation from the samples. Therefore, with fluorescence mode, quantitative information about surface functional groups can be obtained.

In this work, we collected XANES spectra in fluorescence and total electron yield simultaneously and charging effects were closely monitored. Oxygen K-edge XANES analysis was performed on a commercially available activated carbon sample and oxidized activated carbons treated at different temperatures to observe the evolution of the surface functional groups. Oxygen functional group reference compounds were also measured by XANES for both qualitative and quantitative analyses. The identification of surface functional groups on the activated carbon samples and the information about the relative amount of each functional group were obtained by linear combination fitting. The total oxygen contents in the activated carbon samples were determined from the edge step. To prevent spectrum distortion by charging effect, spectra from fluorescence yield were used for data analysis.

Chapter 3 Experimental

3.1 Sample Preparation

3.1.1 Reference Compounds for Oxygen Functional Groups

In this work, reference compounds for oxygen functional groups were used for qualitative and quantitative analyses. The compounds are commercially available aromatic compounds and polymers that have one surface functional group in its structure. All the compounds were used without any further treatment. The functional groups included in the work are carbonyl, aldehyde, carboxylic acid, anhydride, ester, ether, and hydroxyl groups. Table 3.1 shows information about the reference compounds for oxygen functional groups used in the work. The spectra of the reference compounds are used in identifying surface functional groups in the samples by fingerprinting and also in quantification of the surface functional groups by linear combination fitting.

Table 3.1. Oxygen functionality reference compounds

Compound	Structure	Functionality	Supplier	Purity (%)
Anthrone	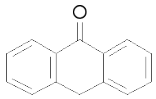	Carbonyl	Alfa Aesar	99
9-Anthraldehyde	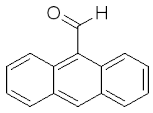	Aldehyde	TCI America	99
1-Naphthoic acid	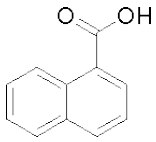	Carboxylic acid	Alfa Aesar	98
Phthalic anhydride	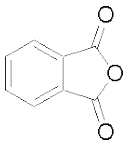	Anhydride	Alfa Aesar	99
Poly(vinyl alcohol) (PVA)	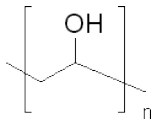	Hydroxyl	Sigma Aldrich	N/A
Poly(4-vinylphenol) (PVP)	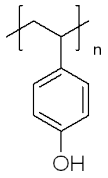	Hydroxyl	Sigma Aldrich	N/A
Poly(acrylic acid) (PAA)	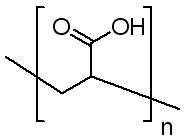	Carboxylic acid	Sigma Aldrich	N/A
Poly(vinyl chloride-co-vinyl acetate) (PVCVA)	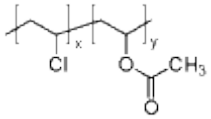	Ester	Sigma Aldrich	N/A
Methyl cellulose	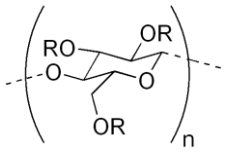	Ether	Sigma Aldrich	N/A

3.1.2 Ammonium Persulfate-treated Activated Carbons

An ultra fine petroleum coke-based activated carbon with a product name AC4 was purchased from Kansai Coke and Chemicals Company Ltd. To demonstrate that surface functional groups can be created by an oxidizer and controlled by thermal treatment, a series of samples were prepared from AC4 by Na Li at the EMS Energy Institute. AC4 activated carbon was treated by a mixture of 1.5 M ammonium persulfate ($(NH_4)_2S_2O_8$) and 1 M sulfuric acid (H_2SO_4). First, one gram of the AC4 activated carbon was mixed with 20 ml of the oxidizer at 60 ^oC in a flask for three hours. The reacted sample was filtered and washed with water, and then dried at 110 ^oC in a vacuum oven overnight. The dried sample was thermally treated at different temperatures (250 and 1050 ^oC) for three hours, under nitrogen atmosphere. Four different activated carbon samples used in this work are referred to as AC4 (untreated activated carbon), OAC4 (oxidized activated carbon), OAC4L (oxidized activated carbon thermally treated at 250 ^oC), and OAC4H (oxidized activated carbon thermally treated at 1050 ^oC).

3.2 Characterization

3.2.1 Oxygen K-edge XANES Spectroscopy

Oxygen K-edge XANES measurements were performed at beamline U4B of the National Synchrotron Light Source (NSLS) at Brookhaven National Laboratory. Detailed information about the experimental setup can be found elsewhere [56]. The storage ring at NSLS was operated with an electron beam energy of 800 MeV and an average current

of 600 mA. XANES spectra were collected in both fluorescence yield and total electron yield modes simultaneously. Multiple scans were taken for each sample, and the spectra were averaged to improve signal to noise ratio. A spectrum of reference material including V, O, and Cr was also collected in every scan for energy alignment. The energy range was from 510 to 590 eV. The energy interval was 0.1 eV in the critical region (from 520 to 560 eV) and 0.5 eV in the other region. Samples were pressed onto a copper tape uniformly, and no cracks observed. The samples were about tenths of a millimeter thick so no signal interference from the adhesive on the copper tape was expected. The samples were placed in an ultra high vacuum chamber maintained at a pressure lower than 10^{-8} Pa. The XANES spectra were processed, and quantitative analysis performed by linear combination fitting using Athena, a free software for XAFS data processing [57].

3.2.2 Temperature Programmed Desorption (TPD-MS)

Temperature-programmed desorption (TPD) analysis of the activated carbon samples was performed on AutoChem 2910 (Micromeritics). 100 mg of each sample was placed in a quartz tube and heated from room temperature to 110 ^{o}C at 5 ^{o}C/min in a vacuum environment. The temperature was maintained at 110 ^{o}C for 1 h in order to remove physisorbed water, and then increased to 1050 ^{o}C under helium (99 %) and argon (1%) atmosphere. The flow rate for the gas mixture was 50 ml/min. The temperature was maintained at 1050 ^{o}C for 1 h. The TPD spectra were corrected by using argon gas as a reference. The evolved gases from samples were analyzed using a quadrupole mass spectrometer (Dycor, Model 2000). To obtain information about surface functional

groups, the collected TPD spectra were analyzed by using the deconvolution parameters from the work of Figueiredo and co-workers [27,40]. Calcium oxalate (CaC_2O_4) was used to calibrate the amounts of CO and CO_2 evolved the samples. As 1 mole of calcium oxalate produce 1 mol of CO and CO_2 when thermally treated, the peak areas of both CO and CO_2 evolved from a series of calcium oxalates with different concentrations were obtained, and the information about the peak areas was used to calculate the absolute amount of oxygen in the activated carbon samples.

3.2.3 Diffuse Reflectance Infrared Fourier Transform Spectroscopy (DRIFTS)

Infrared characterization was performed using FTIR 3000 spectrophotometer with diffuse reflectance cell. Before IR analysis, the activated carbon samples were mixed with potassium bromide (KBr). The mass ratio of an activated carbon sample to KBr was 1:60. The background of IR spectra was measured based on KBr. 400 scans were obtained for each sample with a spectral resolution of 2 cm^{-1}

Chapter 4 Results and Discussions

4.1 Oxygen K-edge XANES Analysis

4.1.1 Total Electron Yield and Fluorescence Yield

Among the standards we have tested, some have good electrical conductivity and do not suffer from charging effect. Figure 4.1 shows the XANES spectra of poly(vinyl alcohol) (PVA) collected in fluorescence yield and total electron yield modes. These are good examples of "normal" XANES spectra. The two spectra are almost identical, so there is no distortion observed due to charging in the total electron yield spectrum. In addition, it can be also seen that self absorption problem is not an issue in this work because there is no intensity reduction in the fluorescence spectrum.

On the contrary, some standards have poor electrical conductivity and suffer adversely from charging effect. Figures 4.2 and 4.3 show XANES spectra of anthraldehyde and anthrone collected in fluorescence yield and total electron yield modes. Severe distortion is observed for anthraldehyde spectrum collected in total electron yield mode. The absorption before pre-edge peak (~536 eV) rapidly decreases with increasing energy, which is not normally expected as suggested by the fluorescence measurement. The valley between pre-edge peak and white line is even lower than the background. The results from fluorescence yield do not suffer from this charging effect, however, it has its own disadvantage. Spectra collected in fluorescence yield mode are intrinsically much noisier. To improve the statistics, multiple scans usually are needed, which increases the experiment time. Figure 4.4 and 4.5 show six scans from poly(4-vinylphenol) and the

result of averaged spectrum. The merged spectrum has an improved signal to noise ratio since signal to noise ratio is improved by the square of the number of merged scans.

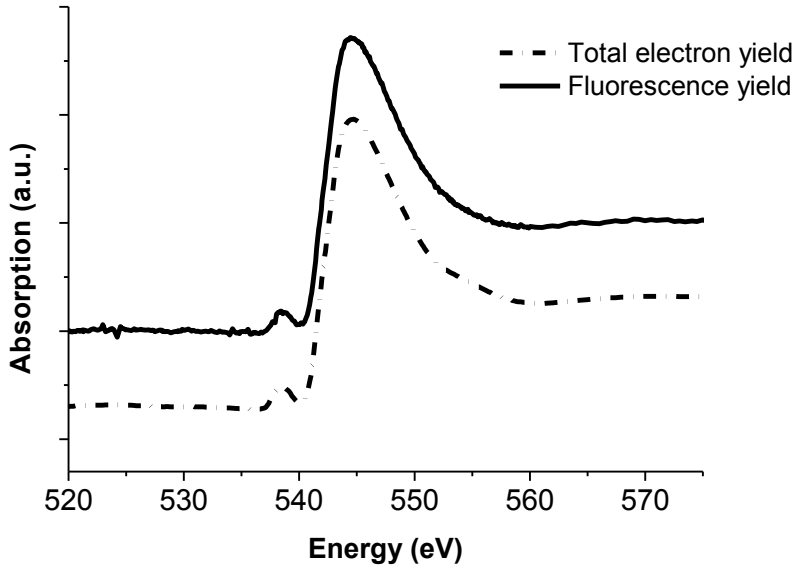

Figure 4.1. XANES spectra of PVA collected in fluorescence yield and total electron yield modes

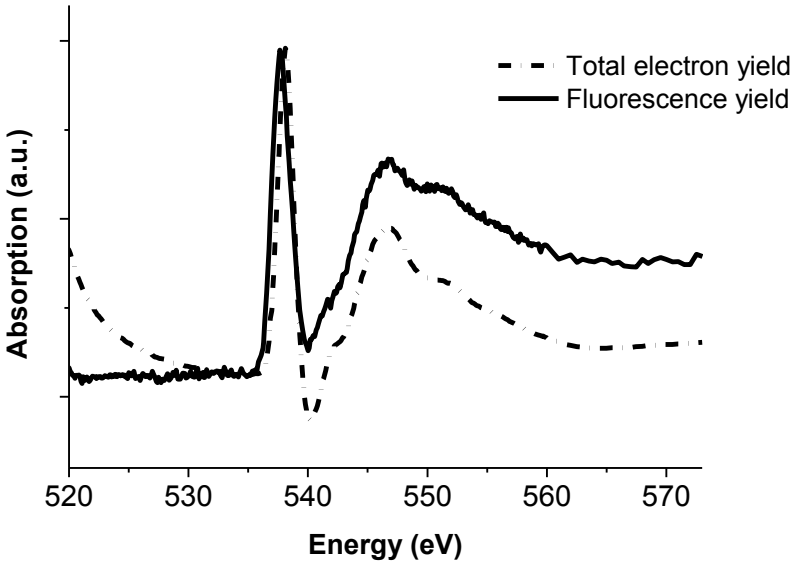

Figure 4.2. XANES spectra of anthraldehyde collected in fluorescence yield and total electron yield modes

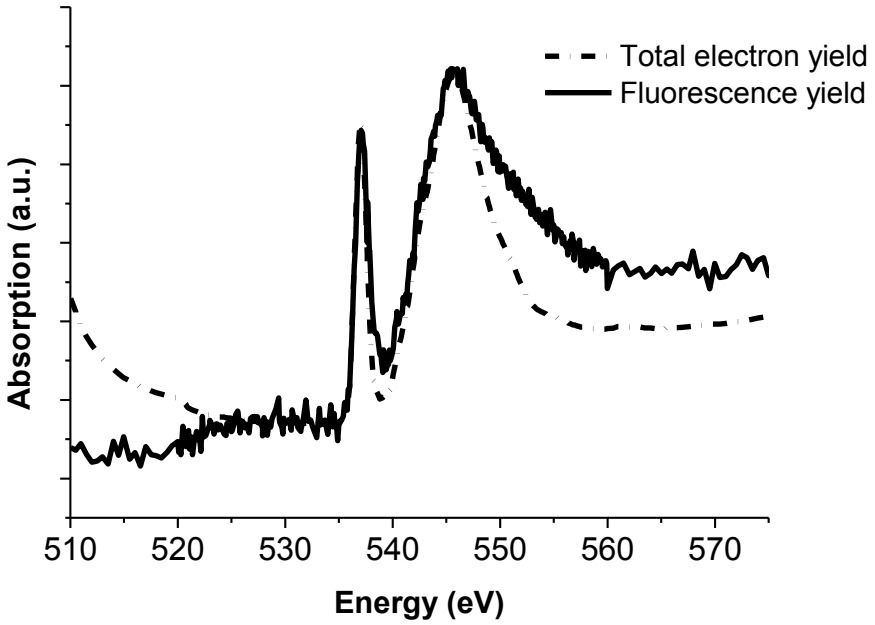

Figure 4.3. XANES spectra of anthrone collected in fluorescence yield and total electron yield modes

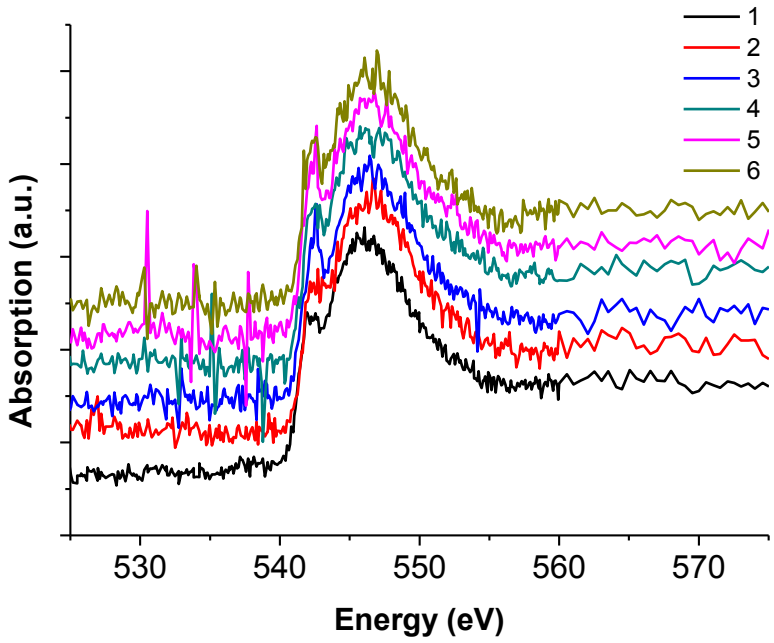

Figure 4.4. Multiple XANES spectra of PVP collected in fluorescence yield mode before merging

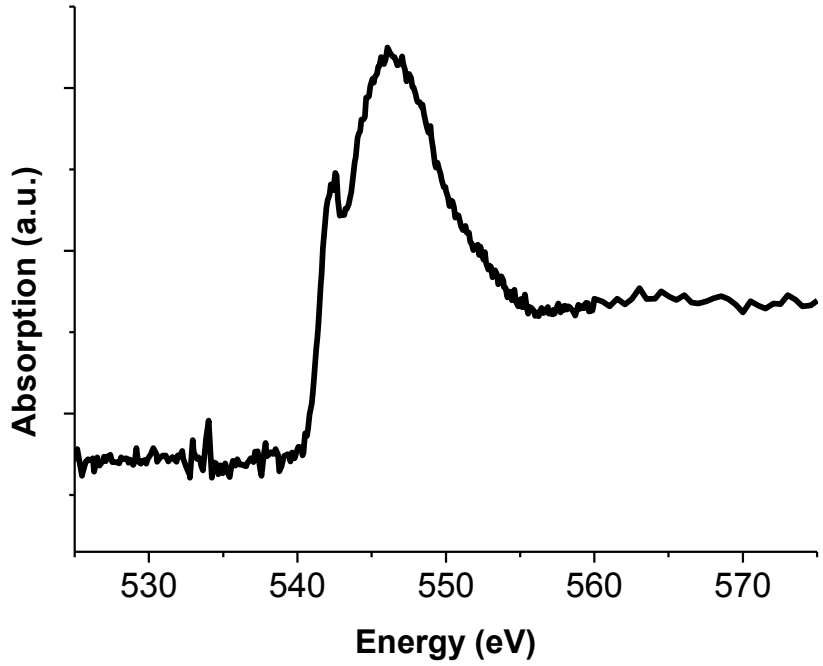

Figure 4.5. Merged XANES spectrum of PVP

4.1.2 XANES Spectra of Individual Functional Groups

XANES spectra of the reference compounds of different functional groups are shown in Figures 4.6, 4.7 and 4.8. All spectra were collected in fluorescence yield mode, and are rescaled for better comparison. As a general observation, oxygen K-edge spectra consist of pre-edge feature (sharp peak around 530 eV) and a broad whiteline (first intense post-edge peak, near 540 eV in this case). Some functional groups have very similar XANES spectra, and are very difficult to discriminate, while some are very different and can be much easier to distinguish. For this reason, functional groups are grouped into three types. Carboxyl-type functional groups include carboxylic acid (PAA and naphthoic acid), anhydride (phthalic anhydride), and ester (PVCVA); hydroxyl-type

functional groups include phenolic hydroxyl (PVP), aliphatic hydroxyl (PVA), and ether (methyl cellulose), and carbonyl-type functional groups include carbonyl (anthrone) and aldehyde (anthraldehyde). As shown in Figure 4.6, carboxyl-type functional groups show a strong pre-edge peak at about 531 eV and a broad whiteline at 539 eV. They also have a small second pre-edge peak at about 533 eV. In contrast, hydroxyl-type functional groups possess no or very weak pre-edge peak at about 531 eV and a broad whiteline at 536-538 eV (see Figure 4.7). Carbonyl-type functional groups, as shown in Figure 4.8, show a strong pre-edge peak below 530 eV and a broad whiteline at 539 eV.

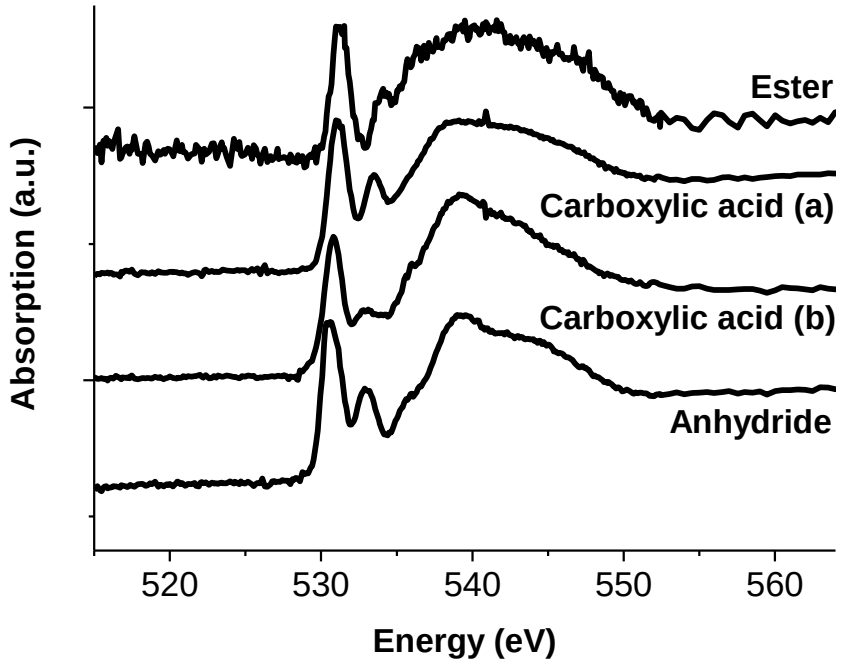

Figure 4.6. Oxygen K-edge XANES spectra of carboxyl-type functional groups: (1) ester (PVCVA), (2) carboxylic acid (a) (PAA), (3) carboxylic acid (b) (naphthoic acid), (4) anhydride (phthalic anhydride)

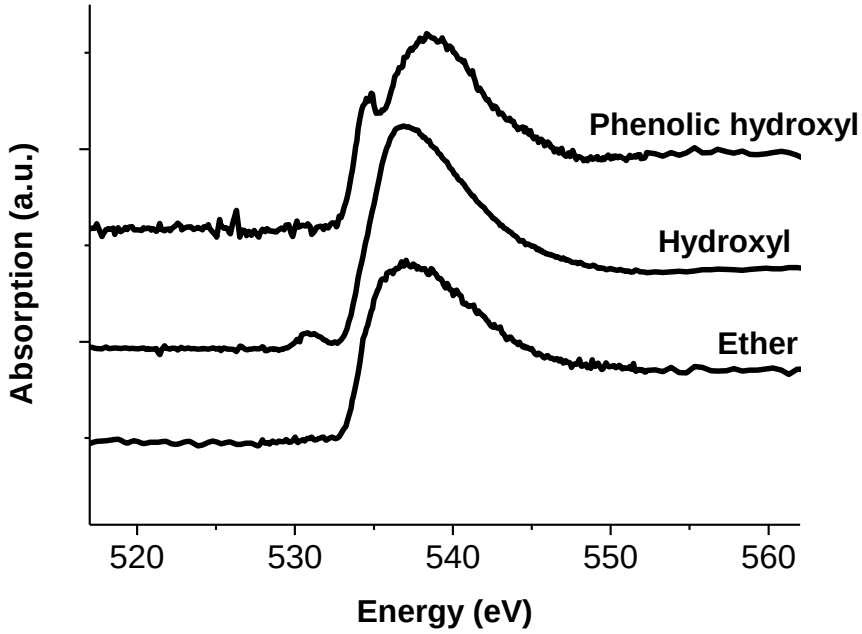

Figure 4.7. Oxygen K-edge XANES spectra of hydroxyl-type functional groups: (1) phenolic hydroxyl (PVP), (2) hydroxyl (PVA), and (3) ether (methyl cellulose)

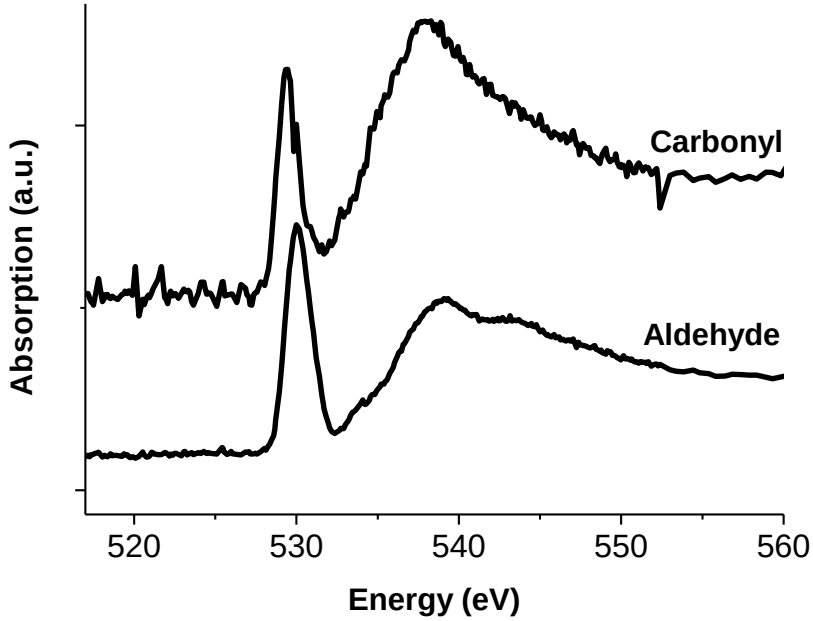

Figure 4.8. Oxygen K-edge XANES spectra of carbonyl-type functional groups: (1) Carbonyl (anthrone), (2) aldehyde (anthraldehyde)

The difference between different types of functional groups is significant. Figure 4.9 presents normalized XANES spectra of the carboxyl, hydroxyl, and carbonyl groups, which manifests differences among them. The main difference lies in the intensity and position of the pre-edge peak. Both carboxyl and carbonyl groups possess intense pre-edge peak with big separation in peak position of about 2 eV. In contrast, hydroxyl-type groups have negligible pre-edge peak and probably the most intense whiteline. The whiteline appears in the lowest energy among all the examined functional groups.

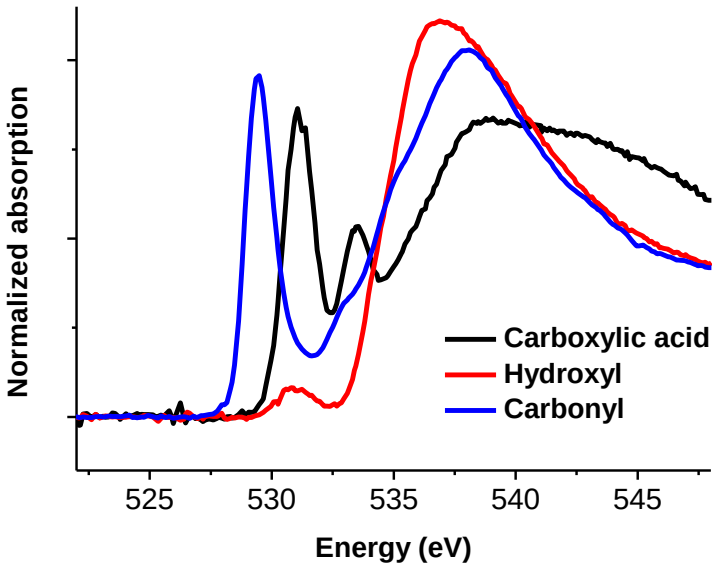

Figure 4.9. Normalized oxygen K-edge XANES spectra of carboxylic acid (PAA), hydroxyl (PVA), and carbonyl (anthrone)

Another important observation is that when same functional groups are situated in different chemical environments, for example, carboxyl groups on a straight hydrocarbon chain (PAA) or aromatic carbon (naphthoic acid), the XANES spectra appear almost the same; the difference due to different chemical environment can be neglected when

compared to the significant differences among the different types of functional groups. Later, when linear combination fitting analysis is performed to quantify different functional groups that are present in a sample, one assumption is that the spectrum of a functional group in reference compound is the same as in the samples (although presumably the chemical environment is different). This is reasonable since XANES spectrum is mainly determined by the direct binding situation around the element of interest. The chemical environment in which a functional group is situated may affect the spectrum a bit, but it is secondary. The assumption is thus strongly supported by the experimental observation.

4.1.3 Ammonium Persulfate-treated Activated Carbons

Figure 4.10 shows oxygen K-edge XANES spectra of AC4, OAC4, OAC4L, and OAC4H. The spectra were collected in fluorescence mode. The peak shape and position suggest that some oxygen functional groups, especially carboxyl, carbonyl, and hydroxyl groups, exist in the samples. For example, the peak at 530 eV in first three activated carbons (AC4, OAC4, and OAC4L) are higher than that of hydroxyl spectrum and wider than those of carbonyl and carboxyl spectra, indicating that the activated carbons contain contributions from both carbonyl and carboxyl groups. The high valley area between the pre-edge peak and white line and the steep slope of the white line show the presence of carboxyl and hydroxyl groups in the first three activated carbons. Meanwhile, the spectrum from OAC4H has relatively low pre-edge peak and low valley region such that it has a hydroxyl group-like spectrum. However, the differences in the width of the pre-

edge peak and the position of the white line distinguish the spectrum from hydroxyl groups, showing that OAC4H has a large amount of hydroxyl groups and a small amount of carbonyl groups on its surface.

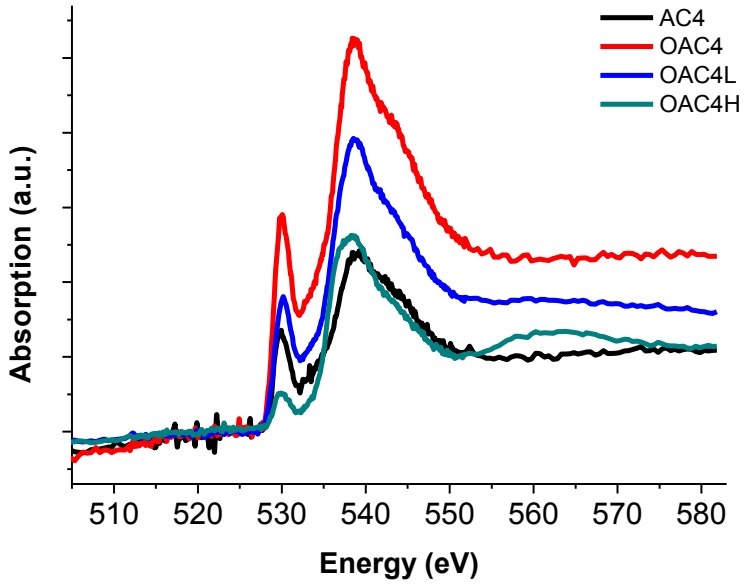

Figure 4.10. Oxygen K-edge XANES spectra of untreated activated carbon (AC4), oxidized activated carbon without heat treatment (OAC4), and thermally treated oxidized activated carbons at 250 ^{o}C and 1050 ^{o}C (OAC4L and OAC4H respectively)

As shown in Figure 4.10, the overall oxygen K-edge x-ray absorption by AC4 greatly increases than OAC4, suggesting that $(NH_4)_2S_2O_8$ indeed oxidized AC4. Moreover, the overall absorption decreases after the thermal treatment, and the higher the treating temperature, the more reduction in absorption. This indicates that the activated carbon loses its oxygen functional groups upon heat treatment. The peak shapes of the spectra also change. For example, the ratio of the pre-edge peak to the white line in OAC4H is much lower than that of OAC4. In addition, the white line of both OAC4L and

OAC4H spectra are shifted to lower energy region. These changes show the *relative* amount (or percentage) of hydroxyl groups within a sample increases as the thermal treatment temperature increases. In addition, the large shift of the white line in OAC4H indicates the greatly increased percentage of hydroxyl groups in OAC4H. In fact, it is shown in the Figure 4.10 that OAC4H has less carbonyl and carboxylic groups than even AC4, but it has more hydroxyl groups. This is probably due to the stability of hydroxyl groups upon the heat treatment. 4.1.4 Total Oxygen Content in the Activated Carbons

It is possible to estimate the total oxygen content in the samples from their oxygen K-edge XANES spectra collected in fluorescence yield mode. According to reference [59], the fluorescence intensity for infinitely thick samples for monochromatic excitation (as in our case) can be expressed as follows,

$$I_i(E_i) = \frac{\eta(E_i)}{4\pi \sin\psi_1} \frac{Q_{if}(E_0) I_0(E_0)}{\mu(E_0)\csc\psi_1 + \mu(E_i)\csc\psi_2} \quad , \qquad (4.1)$$

where E_0 and E_i are the energies of the excitation x-ray and the fluoresced x-ray photons; $I_i(E_i)$ is the intensity of a fluoresced line of energy E_i ; ψ_1 and ψ_2 are the incident angel and outgoing fluorescence angle with regard to the sample surface; μ is the total mass attenuation coefficient; η is the detection efficiency of the x-ray detector for the fluoresced photons at energy E_i; and Q_{if} is the fluorescence probability for measured line from element i .

$$Q_{if}(E_0) = W_i \tau_{Ki}(E_0) \omega_{Ki} f \quad , \qquad (4.2)$$

where W_i is the weight fraction of element i in the sample; τ_{Ki} is the photoelectric mass absorption coefficient for the K shell of element i at the energy E_0; ω_{Ki} is the K-shell

fluorescence yield which describes the fraction of the K shell ionizations that relax by emission of characteristic K-series x-rays; and f, the fraction of monitored fluorescence line in the entire K series in term of intensity.

In our experimental setup, $\psi_1 = \psi_2 = 45°$. For two different activated carbon samples, all parameters are the same except W_i and μ. Substitute Eq. 4.2 into Eq. 4.1 and rearrange, we have:

$$\frac{I_i(E_i)}{I_0(E_0)} = \frac{K\tau_{Ki}(E_0)W_i}{[\mu(E_i)+\mu(E_0)]}, \qquad (4.3)$$

where K is a constant that takes into account factors not related to sample composition. The left term in Eq. 4.3 is how x-ray absorption is measured in fluorescence yield mode. If E_0 is less than the edge energy or the binding energy of K electrons in oxygen (543.1 eV), the fluorescence intensity of K lines is zero; thus the sudden increase in x-ray absorption near the edge (or edge step) is proportional to $\tau_{Ki}(E_0)W_i/[\mu(E_i)+\mu(E_0)]$ for an E_0 that is above the K-edge energy. Since our samples consist of mainly carbon and oxygen (absorption due to H is negligible and assuming no impurities), $\mu = W_i\mu_i + (1-W_i)\mu_C$ (i and c are subscripts for oxygen and carbon, respectively). In addition, τ_{Ki} can be well approximated as $\mu_i(E_0) - \mu_i(E_i)$ as $\mu_i(E_0)$ has contribution from both K and L electrons and for $\mu_i(E_i)$, only L electrons. Thus,

$$\text{Edge step} \propto \frac{KW_i[\mu_i(E_0)-\mu_i(E_i)]}{\{W_i[\mu_i(E_i)+\mu_i(E_0)]+(1-W_i)[\mu_C(E_i)+\mu_C(E_0)]\}}, \qquad (4.4)$$

where E_i = 524.9 eV (energy for oxygen Kα2 line); E_0 is an energy near and above oxygen K-edge energy.

The values of mass absorption coefficient μ for oxygen and carbon are available in Elam database [60], and values at any energy can be calculated using Hephaestus [57]. As shown in figure 4.10, the XANES spectra have no fine structures beyond 575 eV, and the x-ray absorption does not change noticeably. To have a feel of the changing trend of edge step with oxygen weight fraction in carbon materials, we select 580 eV for E_0. The mass absorption coefficients $\mu_i(E_i)$, $\mu_i(E_0)$, $\mu_C(E_i)$, and $\mu_C(E_0)$ are 1293, 17671, 10108, and 11932 cm^2/g, respectively. Substitute the values into Eq. 4.4, we have:

$$\text{Edge step} \propto 0.74KW_i / (1-0.14W_i), \qquad (4.5)$$

Assuming 5% error, when the denominator $1-0.14W_i > 0.95$, we approximate $1-0.14W_i \approx 1$, and edge step becomes proportional to $0.74KW_i$. Thus, if $0.14W_i < 0.05$ or $W_i < 43\%$, the x-ray absorption edge step measured at 580 eV is proportional to the oxygen weight fraction. This condition should be automatically satisfied for most activated carbons.

Table 4.1 shows the edge steps of AC4, OAC4, OAC4L, and OAC4H, and relative oxygen abundance. The edge step of AC4 is assumed to be 1 to calculate the relative oxygen abundance. OAC4 contains the highest oxygen content among the samples, about 2.2 times of AC4. OAC4H contains almost the same amount of oxygen as AC4, indicating that decomposition of surface oxygen functional groups occurred during the heat treatment.

Table 4.1. Edge steps of the activated carbon samples and relative oxygen abundance

Sample	Edge step at 580 eV	Relative Oxygen abundance
AC4	0.107	1.00*
OAC4	0.237	2.21
OAC4L	0.161	1.50
OAC4H	0.113	1.06

* Total oxygen content in AC4 is assumed to be 1.

4.1.4 Linear Combination Fitting

The presence and relative amount of different functional groups in a sample can be obtained by performing linear combination fitting of sample XANES spectrum with the spectra of reference compounds. As discussed in **Section 4.1.2**, the underlying assumption for this operation is that the spectrum of a functional group in reference compound is the same as in the samples, which is supported by the experimental observation. We have also observed that the spectra may shift due to different chemical environments, thus in the fitting process we allow a small energy shift for each reference spectrum to account for the different chemical environments, and the shift must be small (< 0.5 eV) so that there is no crossover between different types of functional groups. Before the analysis is carried out, both sample and reference spectra are normalized to have a common edge step in order to compensate for different oxygen contents among the samples and reference compounds. In the fitting process, the fitting range includes pre-edge and white line. The fitting result of the XANES spectrum is generated by using least-square method. The method minimizes the sum of the squares of the difference

between the value at each data point in the sample spectrum and the calculated value at each data point from linear combination of reference spectra used in the fitting. To find the best fitting result, a large number of different combinations of reference compounds are fitted, and the fitting routine finds the best set of reference compounds and their fractions. The criteria to determine good fitting are R-factor and visual investigation of fitting result especially in the pre-edge region. R-factor is described as

$$\text{R-factor} = \frac{\sum(\text{data - fit})^2}{\sum(\text{data})^2}\ , \qquad (4.6)$$

where the summations are over the data points in the fitting range. Since R-factor shows a deviation of a fitting, a fitting result with the lowest R-factor is considered the best fit. Linear combination fitting provides information about chemical identity of surface functional groups and their relative abundances. In this work, all the data processing and fitting were performed by using Athena [57].

4.1.5 Fitting Results

Figures 4.11 to 4.14 show fitted spectra of the activated carbon samples from linear combination fitting. The fitted results are presented in Tables 4.2 to 4.6 Functional groups of all three types, namely, carboxyl-type, hydroxyl-type, and carbonyl-type, are observed in AC4, OAC4 and OAC4L while OAC4H only contains hydroxyl-type and carbonyl-type functional groups. The absolute uncertainties in the relative abundance are quite small, about 3%. The relative uncertainties (uncertainty divided by fitted abundance) are also small for the major components such as carboxyl-type functional

groups in AC4, OAC4, and OAC4L while it is rather large for the minor component, hydroxyl-type functional groups. Note that the summation of all species is very close to but not exactly 1. The summation is not forced to be 1 because good fits are expected to converge at 1 as we have observed. The small deviation from 1 can easily result from the errors associated with normalization. The relative abundance or percentage of each type of functional groups changes significantly before and after oxidation and heat treatment. In AC4, the most abundant functional groups are carbonyl-type, about 57% (carbonyl + aldehyde), followed by carboxyl-type functional groups, about 41%. The hydroxyl-type functional groups are minor, only about 6%. In OAC4, the most abundant functional groups are carboxyl-type, about 62% (carboxyl + anhydride), followed by carbonyl-type functional groups, about 38%. The hydroxyl-type functional groups are still minor, only about 7%. In OAC4L, carboxyl-type groups are most abundant, about 49%, followed by hydroxyl type-groups, about 32%. Carbonyl-type groups decrease to 18%. In OAC4H, hydroxyl-type groups dominate the sample, about 89%, followed by carbonyl-type groups, about 17%. There is not carboxyl-type functional groups observed in OAC4H. The fitting results confirm that the presence of carbonyl, carboxyl, and hydroxyl groups in AC4, OAC4, and OAC4L and the dominance of hydroxyl groups in OAC4H, which are observed when comparing activated carbon XANES spectra. With information about relative total oxygen content and relative abundance of each surface functional group, it is possible to monitor the evolution of a certain functional group.

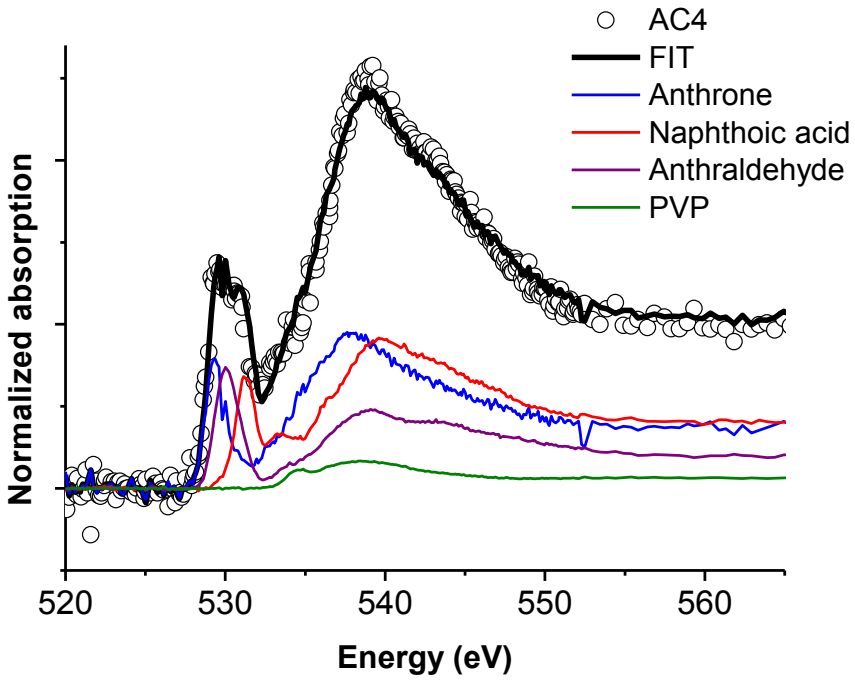

Figure 4.11. Fitting result of AC4 (untreated activated carbon)

Table 4.2. Results from linear combination fitting of AC4 spectrum (uncertainties in parentheses)

Functional group	**Relative abundance (%)**	**Energy shift (eV)**
Carbonyl	37.4 (1.7)	-0.09
Aldehyde	20.1(1.3)	0.00
Carboxylic acid	40.8 (1.4)	0.46
Hydroxyl (phenolic)	6.4 (1.5)	0.00

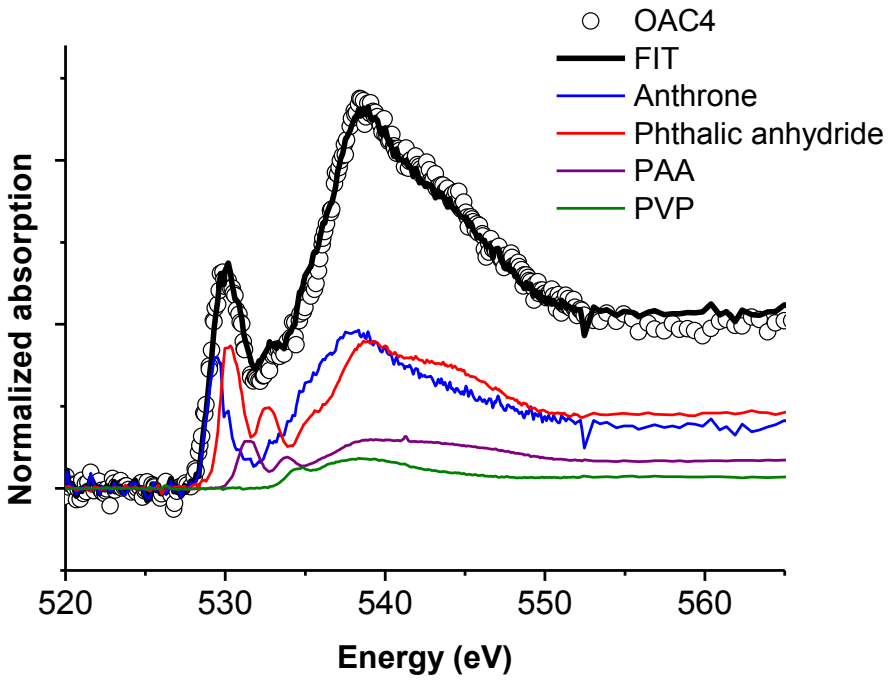

Figure 4.12. Fitting result of OAC4 (oxidized activated carbon without heat treatment)

Table 4.3. Results from linear combination fitting of OAC4 spectrum (uncertainties in parentheses)

Functional group	Relative abundance (%)	Energy shift (eV)
Carbonyl	38.0 (1.5)	-0.04
Anhydride	45.6 (1.8)	-0.33
Carboxylic acid	16.9 (1.7)	0.34
Hydroxyl (phenolic)	7.0 (1.1)	0.00

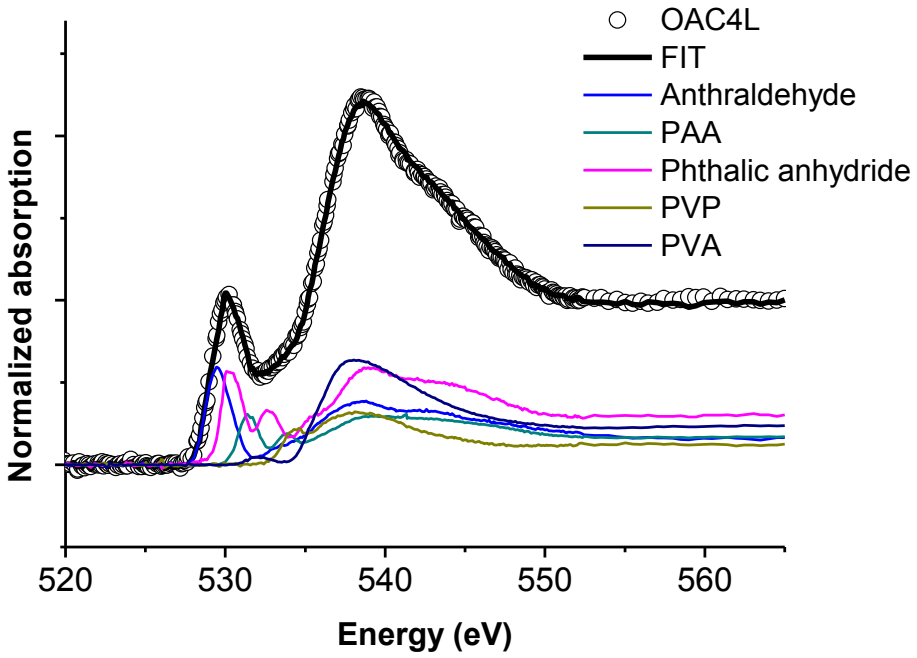

Figure 4.13. Fitting result of OAC4L (oxidized activated carbon treated at 250 ^{o}C)

Table 4.4. Results from linear combination fitting of OAC4L spectrum (uncertainties in parentheses)

Functional group	Relative abundance (%)	Energy shift (eV)
Aldehyde	17.9 (0.8)	-0.495
Anhydride	31.1 (1.7)	-0.219
Carboxylic acid	17.6 (1.5)	0.419
Hydroxyl (phenolic)	32.4 (0.7)	0.209

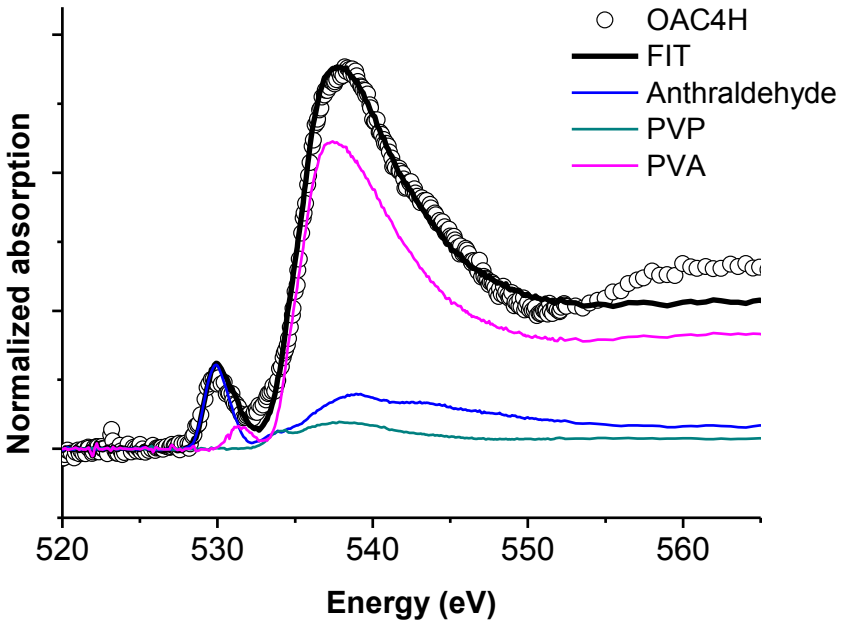

Figure 4.14. Fitting result of OAC4H (oxidized activated carbon treated at 1050 °C)

Table 4.5. Results from linear combination fitting of OAC4H spectrum (uncertainties in parentheses)

Functional group	Relative abundance (%)	Energy shift (eV)
Aldehyde	16.6 (0.8)	-0.156
Hydroxyl (phenolic)	7.4 (2.1)	-0.500
Hydroxyl	81.5 (2.2)	0.500

Table 4.6. Linear combination fitting results of activated carbon samples by XANES

Sample / Functional group	AC4	OAC4	OAC4L	OAC4H
	Relative concentration (%)			
Carbonyl-type*	57.5 (±2.1)	38.0 (±1.5)	17.9 (±0.8)	16.6 (±0.8)
Carboxyl-type**	40.8 (±1.4)	62.5 (±2.5)	48.7 (±2.3)	0
Hydroxyl-type***	6.4 (±1.5)	7.0 (±1.1)	32.4 (±0.7)	88.9 (3.0)
SUM	104.7 (±2.9)	107.5 (±3.1)	99.0 (±2.5)	105.5 (±3.1)
R-factor	2.9×10^{-3}	2.8×10^{-3}	2.4×10^{-3}	5.2×10^{-3}

* includes carbonyl and aldehyde groups

** includes carboxyl acid, ester, and anhydride groups

*** includes hydroxyl (phenolic and aliphatic) and ether groups

The total oxygen contents determined from the x-ray absorption edge step, combined with the relative abundance determined by linear combination fitting for each type of surface functional groups, allows the quantification of different types of functional groups in the samples. The results are presented in Table 4.7. Note that the absolute amount is expressed in terms of the total oxygen content in AC4, which cannot be determined solely by XANES. The absolute amount of each type of functional groups in the activated carbons increases after oxidation. The most created functional groups by oxidation are carboxyl-type. The increase in carboxyl-type functional groups is about 3.5 times that of carbonyl-type or 10 times that of hydroxyl-type functional groups. Meanwhile, heat treatment on the oxidized activated carbon changes the relative abundance of each functional group. While carbonyl-type and carboxyl-type functional groups are reduced during heat treatment at 250 ^{o}C, the amount of hydroxyl-type groups

is 3.5 times that of OAC4. At 1050 ^{o}C, hydroxyl-type groups increase by 6 times compared with OAC4, but the reductions in carbonyl-type and carboxyl groups are significant. The amount of carbonyl-type groups is less than a quarter of that of OAC4, and no carboxyl-type functional groups are detected in OAC4H. These quantitative results strongly support the qualitative discussion of XANES spectra in **section 4.1.3.**

Table 4.7. Absolute content of each type of functional groups in activated carbon samples

Functional group	**AC4***	**OAC4**	**OAC4L**	**OAC4H**
	Absolute oxygen content			
Carbonyl-type	0.55	0.78	0.27	0.17
Carboxyl-type	0.39	1.28	0.74	0
Hydroxyl-type	0.06	0.14	0.49	0.89

*Total oxygen content in AC4 is assumed to be 1.

4.2 TPD Analysis

Figure 4.15 shows deconvolution of temperature-programmed desorption (TPD) pattern of OAC4. Gaussian-Lorentzian mix function and linear background are used, and the maximum limit of full width at half maximum is 150 ^{o}C. The ratio of Gaussian function to Lorentzian function is 70:30. Spectrum deconvolution is performed using the fitting parameters specified in the work of Figueiredo and co-workers [27,40]. The peak at 500 ^{o}C in CO spectrum and peak at 480 ^{o}C in CO_2 spectrum are attributed to anhydride groups. The peak at 640 ^{o}C in CO spectra comes from hydroxyl groups. Carbonyl and/or quinone groups contribute to the two peaks at 810 ^{o}C and 980 ^{o}C in CO spectrum. The

three peaks CO#1, CO#2, and CO#3 in CO spectrum and CO_2#1in CO_2 spectrum have not been clearly assigned yet. In CO_2 spectrum, carboxylic acid groups appear at 280 ^oC and 360 ^oC. The peaks at 640 ^oC and 780 ^oC in CO_2 spectrum are attributed to lactone groups.

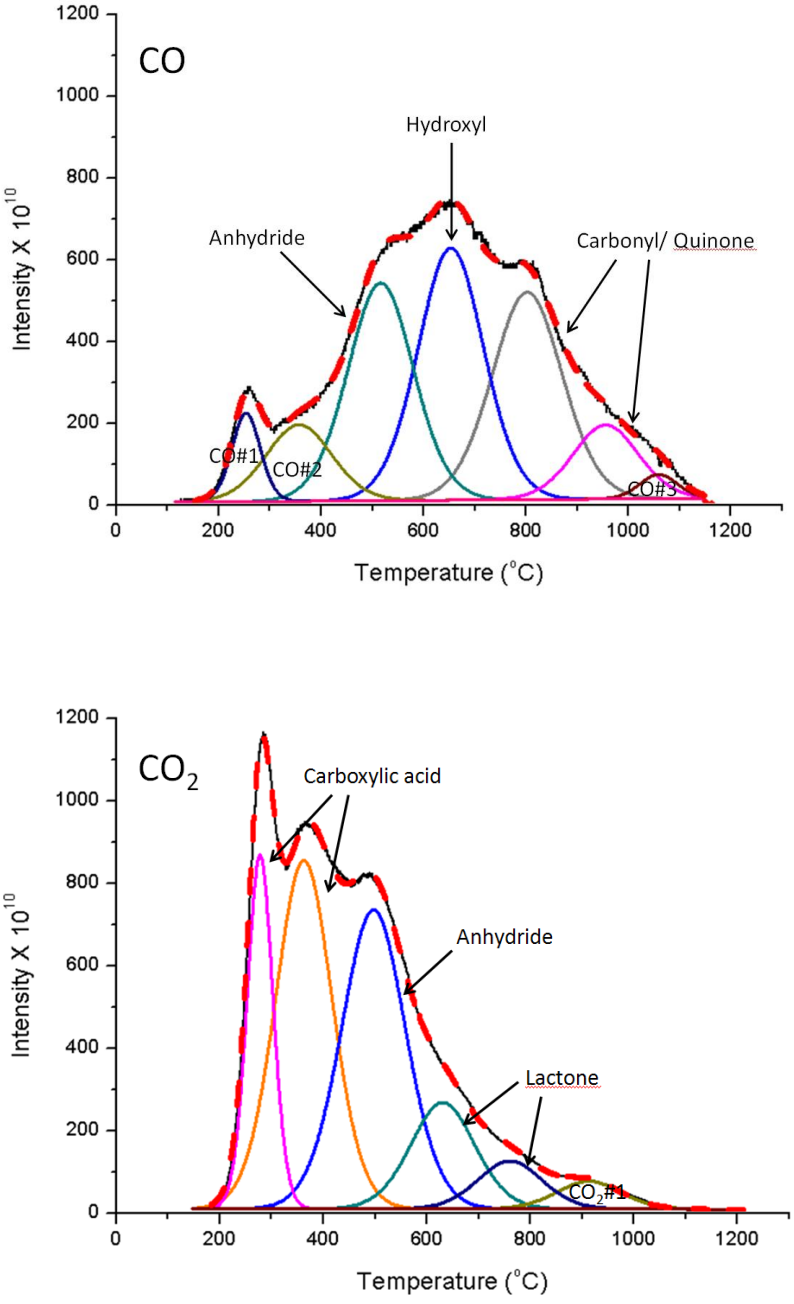

Figure 4.15. Results of deconvolution of TPD spectra from OAC4

Table 4.8 shows total oxygen content in AC4 and OAC4, and absolute abundance of each functional group in the samples. Oxidation by ammonium persulfate greatly increases the amounts of carboxylic acid and anhydride, more than 600 % for both functional groups. Hydroxyl and lactone groups are increased by 207 % and 155 %, respectively. Carbonyl and/or quinone groups are increased by 94%, the least increase among the functional groups. Total oxygen content in AC4 is increased by 290%. Note that the total oxygen content includes the unassigned peaks, CO#1, CO#2, CO#3, and CO_2#1.

Table 4.8. TPD analysis results of AC4 and OAC4

Functionality / Sample	Carbonyl / Quinone	Carboxylic acid	Anhydride	Lactone	Hydroxyl	Total oxygen content (mmol/g)
	Absolute abundance (mmol/g)					
AC4	1.74	0.38	0.18	0.2	1.00	6.25
OAC4	3.38	2.81	1.67	0.51	3.07	24.35
Increase	94 %	639 %	827 %	155 %	207 %	290 %

TPD is useful because it provides not only absolute abundance of surface functional groups, but also total oxygen content in a sample. However, deconvolution result of a TPD spectrum can vary depending on parameters used in the process such as the ratio of Gaussian function to Lorentzian function, full width at half maximum, and peak positions. Figure 4.16 and 4.17 show deconvolution results of OAC4 TPD spectra generated by using different fitting parameters. The parameters employed for the fitting were the same as those used in Figure 4.15 except that there was no preset constraint for

full width at half maximum. The overall fitting quality is almost the same as shown in Figure 4.15. However, there are noticeable differences in the peak intensities and peak positions. For example, the intensity of anhydride peak at 510 eV in Figure 4.16 is lower than that of Figure 4.15, and the hydroxyl peak at 690 eV in Figure 4.16 is higher and broader than that of Figure 4.15. A new peak shows up at 350 eV between two carboxylic acids in Figure 4.17. In addition, a broader and higher peak appears at 630 eV in Figure 4.17 instead of two lactone peaks in Figure 4.15. The significant difference in deconvolution results from slightly different fitting parameters manifests the sensitivity of TPD characterization of surface functional groups to the selection of fitting parameters. A robust rule of parameter selection should be developed to ensure the reliability of the TPD analysis.

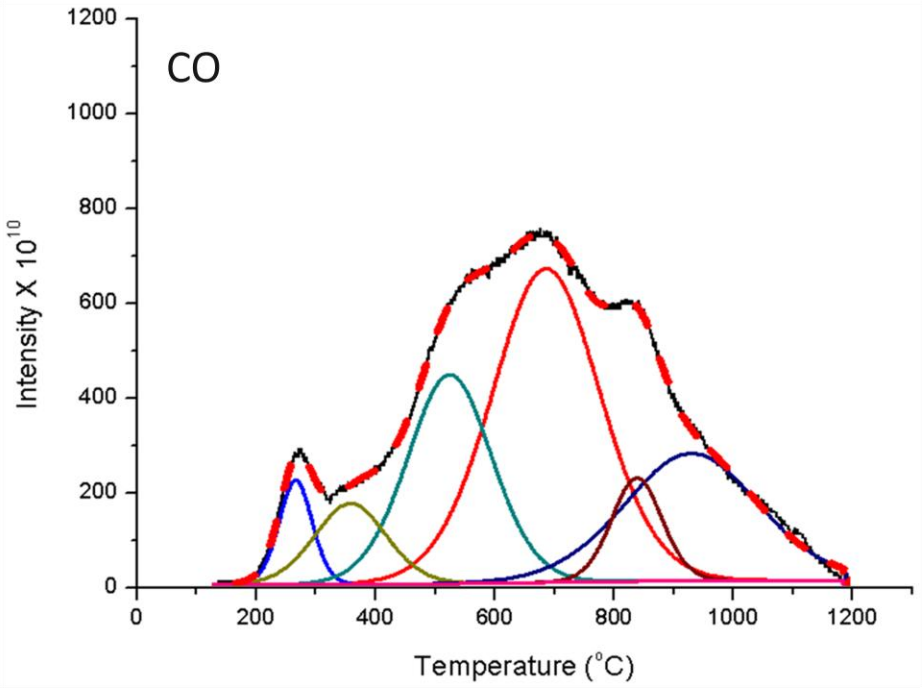

Figure 4.16. Results of deconvolution of TPD spectra (CO) from OAC4 without preset constraint for full width at half maximum

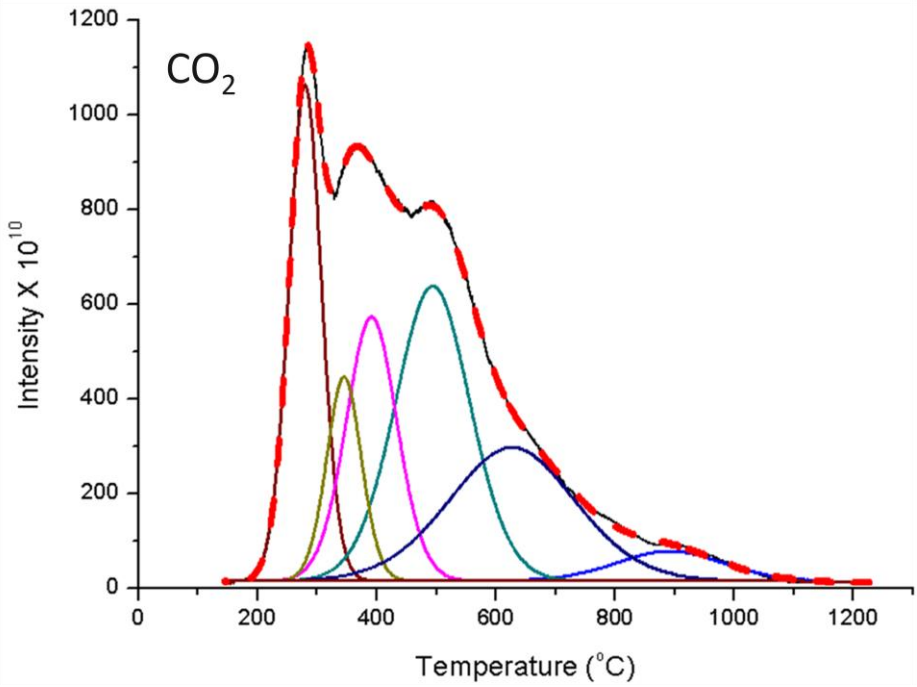

Figure 4.17. Results of deconvolution of TPD spectra (CO_2) from OAC4 without preset constraint for full width at half maximum

4.3 DRIFTS Analysis

Figure 4.18 shows the IR spectra from untreated activated carbon and oxidized activated carbon without heat treatment. Peak assignment is also presented. Peaks are assigned according to the work of Vannice and co-workers [61,62]. The peak appears at 1735 cm^{-1} has contributions from C=O in lactone, carboxylic acid, and anhydride groups. The peak at 1600 cm^{-1} is known to be related to quinone and ceto-enol groups. The most intense peak at 1235 cm^{-1} has contributions from C-O in ether, lactone, phenol, and anhydride groups. It can be seen from the spectra that oxidation of activated carbon with ammonium persulfate greatly increases surface oxygen functional groups. However,

detailed qualitative and quantitative analyses are not possible since each peak has contributions from multiple surface functional groups.

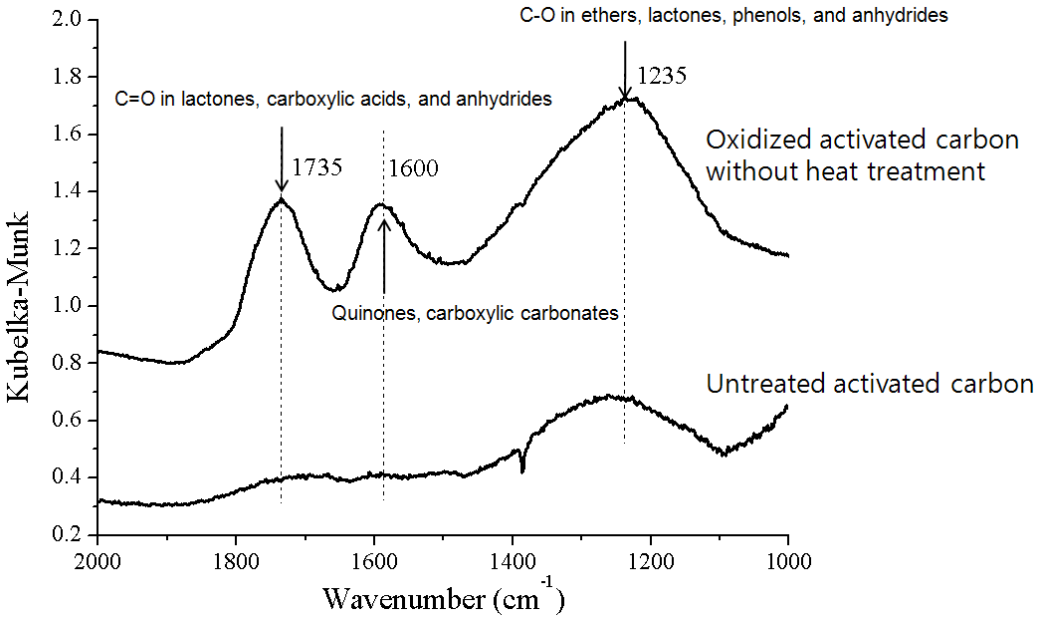

Figure 4.18. Peak assignments of DRIFTS results from untreated activated carbon and oxidized activated carbon without heat treatment

Conclusions and Future Work

Summary and Conclusions

Oxygen K-edge XANES was performed to identify and quantify the surface functional groups on oxidized activated carbons thermally treated at different temperatures. It is shown that the unique spectrum of each type of functional groups (carbonyl, carboxyl, and hydroxyl-type) can be distinguished with XANES. The reliability of XANES analysis lies in the fact that XANES spectroscopy measures the electronic structure near the element of interest, which is dominantly determined by the configuration in the local molecular structure. The unique XANES spectra for different types of functional groups affirm the reliable identification and quantification of the functional groups

The total oxygen contents in a series of samples can be determined from the x-ray absorption edge step since it is proportional to the edge step within a certain oxygen concentration, which can be satisfied in most cases. The precedent oxygen K-edge XANES work which was done 13 years ago was not able to obtain quantitative information because of peak distortion by charging effect due to poor conductivity of carbon materials. In this work, charging effect was closely monitored by collecting data using fluorescence yield and total electron yield modes simultaneously.

Linear combination fitting of XANES spectra of activated carbon samples with reference compounds spectra was performed for both qualitative and quantitative analyses. The assumption that the spectrum of a functional group in reference compound

is the same as in the samples, is strongly supported by the experimental observation. From linear combination fitting, surface functional groups in a sample can be identified, and their relative abundance (percentage) can be determined. The fitting results show that the oxidation of activated carbon by ammonium persulfate not only increases the amount of oxygen in the samples, but also changes the relative abundance of surface functional groups. The oxygen content of the oxidized activated carbons decreases when thermally treated, and at higher temperature, the oxygen loss is significant such that the total oxygen content becomes similar to that of untreated activated carbon. Although the untreated activated carbon and the thermally treated activated carbon contains similar amount of oxygen, relative abundance of each functional group in the samples are quite different. After the heat treatment, the concentration of hydroxyl-type groups greatly increases, while those of carbonyl-type and carboxylic-type groups decrease. With all the qualitative and quantitative information provided from XANES, one can follow the evolution of a certain functional group during heat treatment.

TPD and DRIFTS were also performed on untreated activated carbon and oxidized activated carbon to see the effect of ammonium persulfate on surface functional groups. It is shown in the results from both techniques that oxidation with ammonium persulfate greatly increased the surface functional groups. TPD results provide the absolute quantity of each surface functional group and total oxygen content in a sample. However, deconvolution result of TPD spectrum is strongly influenced fitting parameters. This may decrease the reliability of the technique. Although DRIFTS is useful to follow changes in a series of samples, detailed qualitative and quantitative analyses are

significantly hindered because each peak contains contributions from multiple functional groups.

Carbon materials allow a variety of potential applications which will certainly lead us to improved technologies. To take full advantage of these potentials, careful investigation of the surface chemistry of carbon materials is of most importance since their properties are strongly influenced by functional groups on the surface. The limitations of conventional characterization methods on identification and quantification have raised the need for new methods, and XANES is a good candidate. Although it is not possible to solve all the problems only with XANES, the information obtained is very useful and can be even strengthened when used in combination with other methods.

Future Work

In this work, we examined activated carbon samples by XANES. XANES can be applied to study many other carbon materials to identify the nature of surface functional groups and their relative abundance. This will help understand the properties of carbon materials. For example, soot is a collection of hazardous carbonaceous particulate matters produced by the imperfect combustion of hydrocarbon. Oxidation of soot plays a significant role in reducing human health problems caused by particulate emissions. However, the oxidation mechanism of soot is not fully understood. Since reactivity of carbon materials is dependent strongly on their surface chemistry, characterizing surface functional groups of soot can suggest proper chemical mechanisms for soot oxidation. XANES can also be applied to study carbon deposition of metal oxide supported metal

catalysts. Since the metal substrate also contains oxygen in metal oxide form, both carbon and oxygen K-edge spectra will be measured to identify the carbon species on the catalysts.

Since XANES is not as widely available as other techniques, it may work as a calibration tool for other techniques. This can resolve inconsistencies of characterization results that sometimes occur among different characterization techniques.

Since XANES can provide information about identity and relative abundance of surface functional groups, it can be used to measure the surface functional group dependence of the performance of carbon materials. For example, with quantitative and qualitative information about surface functional groups on activated carbons, their adsorption behaviors toward many different pollutants can be elucidated, and this will help produce an effective and efficient adsorbent for a specific pollutants.

References

[1] A. D. McNaught, A. Wilkinson editors. IUPAC. Compendium of Chemical Terminology, 2nd ed. (the "Gold Book"), Diamond. Oxford: Blackwell Scientific Publications; 1997.

[2] A. D. McNaught, A. Wilkinson editors. IUPAC. Compendium of Chemical Terminology, 2nd ed. (the "Gold Book"), Graphite. Oxford: Blackwell Scientific Publications; 1997.

[3] Singh R, Pantarotto D, Lacerda L, Pastorin G, Klumpp C, Prato M, et al. Tissue biodistribution and blood clearance rates of intravenously administered carbon nanotube radiotracers. Proc.Natl.Acad.Sci.U.S.A. 2006 02/28;103(9):3357-62.

[4] Baibarac M, Gomez-Romero P. Nanocomposites based on conducting polymers and carbon nanotubes: from fancy materials to functional applications. Journal of Nanoscience and Nanotechnology 2006 02;6(2):289-302.

[5] Yue ZR, Jiang W, Wang L, Gardner SD, Pittman Jr. CU. Surface characterization of electrochemically oxidized carbon fibers. Carbon 1999;37(11):1785-96.

[6] Klein KL, Melechko AV, McKnight TE, Retterer ST, Rack PD, Fowlkes JD, et al. Surface characterization and functionalization of carbon nanofibers. J.Appl.Phys. 2008;103(6).

[7] Javey A, Guo J, Wang Q, Lundstrom M, Dai H. Ballistic carbon nanotube field-effect transistors. Nature 2003;424(6949):654-7.

[8] Yu M, Lourie O, Dyer MJ, Moloni K, Kelly TF, Ruoff RS. Strength and breaking mechanism of multiwalled carbon nanotubes under tensile load. Science 2000;287(5453):637-40.

[9] Baker SE, Tse K, Hindin E, Nichols BM, Clare TL, Hamers RJ. Covalent functionalization for biomolecular recognition on vertically aligned carbon nanofibers. Chemistry of Materials 2005;17(20):4971-8.

[10] Baker SE, Colavita PE, Tse K, Hamers RJ. Functionalized vertically aligned carbon nanofibers as scaffolds for immobilization and electrochemical detection of redox-active proteins. Chemistry of Materials 2006;18(18):4415-22.

[11] Fletcher BL, McKnight TE, Melechko AV, Simpson ML, Doktycz MJ. Biochemical functionalization of vertically aligned carbon nanofibres. Nanotechnology 2006;17(8):2032-9.

[12] McKnight TE, Peeraphatdit C, Jones SW, Fowlkes JD, Fletcher BL, Klein KL, et al. Site-specific biochemical functionalization along the height of vertically aligned carbon nanofiber arrays. Chemistry of Materials 2006;18(14):3203-11.

[13] Liu Y, Vander Wal RL, Khabashesku VN. Functionalization of carbon nano-onions by direct fluorination. Chemistry of Materials 2007;19(4):778-86.

[14] Li B, Shi Z, Lian Y, Gu Z. Aqueous Soluble Single-Wall Carbon Nanotube. Chem.Lett. 2001;30(7):598-9.

[15] Zhao W, Song C, Pehrsson PE. Water-soluble and optically pH-sensitive single-walled carbon nanotubes from surface modification. J.Am.Chem.Soc. 2002;124(42):12418-9.

[16] Organic functionalized carbon nanotubes. 16th International Winterschool on Electronic Properties of Novel Materials; 2-9 March 2002; USA: AIP; 2002.

[17] Zhao B, Hu H, Yu A, Perea D, Haddon RC. Synthesis and characterization of water soluble single-walled carbon nanotube graft copolymers. J.Am.Chem.Soc. 2005;127(22):8197-203.

[18] Toebes ML, Van Heeswijk JMP, Bitter JH, Jos vD, De Jong KP. The influence of oxidation on the texture and the number of oxygen-containing surface groups of carbon nanofibers. Carbon 2004;42(2):307-15.

[19] Lakshminarayanan PV, Toghiani H, Pittman CU, J. Nitric acid oxidation of vapor grown carbon nanofibers. Carbon 2004;42(12-13):2433-42.

[20] Lu Y, Xu B, Wang X. Surface modification of polyacrylonitrile-based carbon fiber and its interaction with imide. Appl.Surf.Sci. 2006 12/30;253(5):2695-701.

[21] Rangel-Mendez J, Streat M. Adsorption of cadmium by activated carbon cloth: Influence of surface oxidation and solution pH. Water Res. 2002;36(5):1244-52.

[22] Jiang Z, Liu Y, Sun X, Tian F, Sun F, Liang C, et al. Activated carbons chemically modified by concentrated H2SO4 for the adsorption of the pollutants from wastewater and the dibenzothiophene from fuel oils. Langmuir 2003;19(3):731-6.

[23] Chen JP, Wu S. Acid/Base-Treated Activated Carbons: Characterization of Functional Groups and Metal Adsorptive Properties. Langmuir 2004;20(6):2233-42.

[24] Kundu S, Wang Y, Xia W, Muhler M. Thermal stability and reducibility of oxygen-containing functional groups on multiwalled carbon nanotube surfaces: a quantitative high-resolution XPS and TPD/TPR study. Journal of Physical Chemistry C 2008 10/30;116(43):16869-78.

[25] Boehm HP. Surface oxides on carbon and their analysis: a critical assessment. Carbon 2002 2;40(2):145-9.

[26] Langley LA, Villanueva DE, Fairbrother DH. Quantification of surface oxides on carbonaceous materials. Chemistry of Materials 2006;18(1):169-78.

[27] Figueiredo JL, Pereira MFR, Freitas MMA, Orfao JJM. Characterization of Active Sites on Carbon Catalysts. Ind Eng Chem Res 2007 06/01;46(12):4110-5.

[28] Yamazaki S, Siroma Z, Ioroi T, Yasuda K, Tanimoto K. An electrochemical method for determining the number of carboxyl groups on carbon black. J Electroanal Chem 2008;616(1-2):64-70.

[29] Bajt S, Sutton SR, Delaney JS. X-ray microprobe analysis of iron oxidation states in silicates and oxides using X-ray absorption near edge structure (XANES). Geochim.Cosmochim.Acta 1994;58(23):5209-.

[30] Chen Y, Xie C, Li Y, Song C, Bolin TB. Sulfur poisoning mechanism of steam reforming catalysts: an X-ray absorption near edge structure (XANES) spectroscopic study. Physical Chemistry Chemical Physics 2010;12(21):5707-11.

[31] Turner JA, Thomas KM, Russell AE. Identification of oxygen functional groups in carbonaceous materials by oxygen K-edge XANES. Carbon 1997;35(7):983-92.

[32] Braun A, Huggins FE, Shah N, Chen Y, Wirick S, Mun SB, et al. Advantages of soft X-ray absorption over TEM-EELS for solid carbon studies-a comparative study on diesel soot with EELS and NEXAFS. Carbon 2005;43(1):117-24.

[33] Braun A, Shah N, Huggins FE, Kelly KE, Sarofim A, Jacobsen C, et al. X-ray scattering and spectroscopy studies on diesel soot from oxygenated fuel under various engine load conditions. Carbon 2005;43(12):2588-99.

[34] Braun A, Mun BS, Huggins FE, Huffman GP. Carbon speciation of diesel exhaust and urban particulate matter NIST standard reference materials with C(1s) NEXAFS spectroscopy. Environ.Sci.Technol. 2007 JAN 1;41(1):173-8.

[35] Braun A. Comment on "Effects of Native Organic Material and Water on Sorption Properties of Reference Diesel Soot". Environ.Sci.Technol. 2009 JUL 1;43(13):5158-9.

[36] Lee DW, De Los Santos L, V., Seo JW, Felix LL, Bustamante D A, Cole JM, et al. The Structure of Graphite Oxide: Investigation of Its Surface Chemical Groups. J Phys Chem B 2010 MAY 6;114(17):5723-8.

[37] Skoog DA, Holler FJ, Nieman TA. Principles of instrumental analysis. Fifth ed. USA: BROOKS/COLE; 1998.

[38] Stein A, Wang Z, Fierke MA. Functionalization of Porous Carbon Materials with Designed Pore Architecture. Adv Mater 2009;21(3):265-93.

[39] Seong HJ. Impact of oxygen enrichment on soot properties and soot oxidative reactivity. 2010;.

[40] Figueiredo JL, Pereira MFR, Freitas MMA, Orfao JJM. Modification of the surface chemistry of activated carbons. Carbon 1999;37(9):1379-89.

[41] Wepasnick KA, Smith BA, Bitter JL, Fairbrother DH. Chemical and structural characterization of carbon nanotube surfaces. Anal.Bioanal.Chem. 2010 FEB;396(3):1003-14.

[42] Wildgoose GG, Abiman P, Compton RG. Characterising chemical functionality on carbon surfaces. Journal of Materials Chemistry 2009 07/28;19(28):4875-86.

[43] Yu X, Hantsche H. Some Aspects of the Charging Effect in Monochromatized Focused Xps. Fresenius J.Anal.Chem. 1993 MAY;346(1-3):233-6.

[44] Budinova T, Ekinci E, Yardim F, Grimm A, Björnbom E, Minkova V, et al. Characterization and application of activated carbon produced by H3PO4 and water vapor activation. Fuel Process Technol 2006 10;87(10):899-905.

[45] Kim UJ, Furtado CA, Liu X, Chen G, Eklund PC. Raman and IR spectroscopy of chemically processed single-walled carbon nanotubes. J.Am.Chem.Soc. 2005;127(44):15437-45.

[46] Almarri MS. Selective adsorption for removal of nitrogen compounds from hydrocarbon streams over carbon-based adsorbents. 2009;.

[47] Zhou J, Sui Z, Zhu J, Li P, Chen D, Dai Y, et al. Characterization of surface oxygen complexes on carbon nanofibers by TPD, XPS and FT-IR. Carbon 2007 4;45(4):785-96.

[48] Bandosz TJ, Jagiello J, Contescu C, Schwarz JA. Characterization of the Surfaces of Activated Carbons in Terms of their Acidity Constant Distributions. Carbon 1993;31(7):1193-202.

[49] Stohr J editor. NEXAFS Spectroscopy. Second ed. : Springer; 2003.

[50] Mukerjee S, Srinivasan S, Soriaga MP, Mcbreen J. Role of Structural and Electronic-Properties of Pt and Pt Alloys on Electrocatalysis of Oxygen Reduction - an In-Situ Xanes and Exafs Investigation. J.Electrochem.Soc. 1995 MAY;142(5):1409-22.

[51] Lamberti C, Bordiga S, Bonino F, Prestipino C, Berlier G, Capello L, et al. Determination of the oxidation and coordination state of copper on different Cu-based

catalysts by XANES spectroscopy in situ or in operando conditions. Physical Chemistry Chemical Physics 2003;5(20):4502-9.

[52] Strange RW, Blackburn NJ, Knowles PF, Hasnain SS. X-ray absorption spectroscopy of metal-histidine coordination in metalloproteins. Exact simulation of the EXAFS of tetrakis (imidazole) copper (II) nitrate and other copper-imidazole complexes by the use of a multiple-scattering treatment. J.Am.Chem.Soc. 1987 11/11;109(23):7157-62.

[53] Rockenberger J, zum Felde U, Tischer M, Troger L, Haase M, Weller H. Near edge X-ray absorption fine structure measurements (XANES) and extended x-ray absorption fine structure measurements (EXAFS) of the valence state and coordination of antimony in doped nanocrystalline SnO2. J.Chem.Phys. 2000 MAR 1;112(9):4296-304.

[54] Troger L, Arvanitis D, Baberschke K, Michaelis H, Grimm U, Zschech E. Full Correction of the Self-Absorption in Soft-Fluorescence Extended X-Ray-Absorption Fine-Structure. Physical Review B 1992 AUG 1;46(6):3283-9.

[55] Cros A. Charging Effects in X-Ray Photoelectron-Spectroscopy. Journal of Electron Spectroscopy and Related Phenomena 1992 JUN 15;59(1):1-14.

[56] Chen CT, Sette F. Performance of the Dragon Soft-X-Ray Beamline. Rev.Sci.Instrum. 1989 JUL;60(7):1616-21.

[57] Ravel B, Newville M. ATHENA, ARTEMIS, HEPHAESTUS: data analysis for X-ray absorption spectroscopy using IFEFFIT. Journal of Synchrotron Radiation 2005 JUL;12:537-41.

[58] McCallum CL, Bandosz TJ, McGrother SC, Muller EA, Gubbins KE. A molecular model for adsorption of water on activated carbon: Comparison of simulation and experiment. Langmuir 1999 JAN 19;15(2):533-44.

[59] Jenkins R, Gould RW, Gedcke D editors. Quantitative X-ray Spectrometry. Second ed. New York: Dekker; 1995.

[60] Elam WT, Ravel BD, Sieber JR. A new atomic database for X-ray spectroscopic calculations. Radiat.Phys.Chem. 2002;63(2):121-8.

[61] Fanning PE, Vannice MA. A Drifts Study of the Formation of Surface Groups on Carbon by Oxidation. Carbon 1993;31(5):721-30.

[62] Dandekar A, Baker RTK, Vannice MA. Characterization of activated carbon, graphitized carbon fibers and synthetic diamond powder using TPD and drifts. Carbon 1998;36(12):1821-31.